UCRL-19128

c.2

DIFFUSION IN CONCENTRATED ELECTROLYTIC SOLUTIONS

Kemal Nisancioglu
(M.S. Thesis)

January 1970

AEC Contract No. W-7405-eng-48

TWO-WEEK LOAN COPY

This is a Library Circulating Copy
which may be borrowed for two weeks.
For a personal retention copy, call
Tech. Info. Division, Ext. 5545

LAWRENCE RADIATION LABORATORY
UNIVERSITY of CALIFORNIA BERKELEY

UCRL-19128

DISCLAIMER

This document was prepared as an account of work sponsored by the United States Government. While this document is believed to contain correct information, neither the United States Government nor any agency thereof, nor the Regents of the University of California, nor any of their employees, makes any warranty, express or implied, or assumes any legal responsibility for the accuracy, completeness, or usefulness of any information, apparatus, product, or process disclosed, or represents that its use would not infringe privately owned rights. Reference herein to any specific commercial product, process, or service by its trade name, trademark, manufacturer, or otherwise, does not necessarily constitute or imply its endorsement, recommendation, or favoring by the United States Government or any agency thereof, or the Regents of the University of California. The views and opinions of authors expressed herein do not necessarily state or reflect those of the United States Government or any agency thereof or the Regents of the University of California.

TABLE OF CONTENTS

ABSTRACT

I. INTRODUCTION ---------- 1

II. A SURVEY OF THE FUNDAMENTALS OF MASS TRANSPORT IN CONCENTRATED ELECTROLYTIC SOLUTIONS ---------- 4

III. METHODS OF CORRELATING AND PREDICTING DIFFUSIVITIES ---------- 9

A. Predicting Diffusivities from Viscosity and Activity Coefficient Data ---------- 9

B. Development of a One Parameter Equation for the Diffusion Coefficient ---------- 27

C. Extention of the Rate Equation ---------- 46

IV. A METHOD FOR THE MEASUREMENT OF DIFFUSIVITY RESTRICTED DIFFUSION - 58

A. Analysis of Restricted Diffusion ---------- 59

B. Analysis of Rayleigh Interference ---------- 63

V. EXPERIMENTAL WORK ---------- 66

A. Description of the Apparatus ---------- 66

1. Optical System ---------- 66

2. Optical Cells ---------- 68

3. Boundary Forming Apparatus ---------- 70

4. Miscellaneous Apparatus ---------- 71

B. Experimental Procedure ---------- 71

1. Diffusion Runs ---------- 71

2. Data Evaluation ---------- 76

C. Results and Discussion ---------- 77

1. Differential Diffusion Coefficients ---------- 77

2. Viscosities ---------- 83

3. Ionic and Thermodynamic Diffusion Coefficients ---------- 85

VI. CONCLUSIONS AND RECOMMENDATIONS ---------- 93

APPENDIX: Functions Used to Fit Thermodynamic and Transport Property Data on Electrolytic Solutions ---------- 97

NOMENCLATURE ---------- 103

ACKNOWLEDGEMENTS ---------- 107

REFERENCES ---------- 108

DIFFUSION IN CONCENTRATED ELECTROLYTIC SOLUTIONS

Kemal Nisancioglu

Inorganic Materials Research Division, Lawrence Radiation Laboratory
Department of Chemical Engineering, University of California
Berkeley, California

ABSTRACT

The analysis of mass transfer problems in electrochemical systems requires accurate values of the transport properties of electrolytic solutions. We study here some methods for the correlation, prediction and measurement of diffusion coefficients in concentrated electrolytic solutions.

We propose a one parameter rate equation, based on a simple lattice model to describe the microstructure of an electrolytic solution, for the diffusion coefficient. We discuss the possibility of estimating diffusivities from viscosity and activity coefficient data. The calculated diffusion coefficients show a fair agreement with the reported experimental values.

Our theoretical study indicates the necessity of obtaining additional experimental data on the diffusion coefficient and viscosity of electrolytic solutions. We measure the viscosity of aqueous nitric acid at 25°C for concentrations 0 to 1.0 molar in order to complement available data on this property. We obtain the differential diffusion coefficients of the same system for the concentration range .033 to 9.25 molar via restricted diffusion. The experimental method employs Rayleigh interferometry to observe a concentration profile and appears to be accurate to 0.2 percent. The experimental results are found to be in qualitative agreement with the behavior of strong acids in aqueous solutions and support the hypotheses concerning the effects of strong acids on the molecular structure of water.

I. INTRODUCTION

Various mass transfer problems are frequently encountered in the analysis, design and control of most electrochemical systems. The solution of such problems requires a systematic description of the fluxes of different species involved and their transport properties. Information about the transport properties can be gathered from experimental data or from theories describing the nature of electrolytic systems on the microscopic scale. Several such theories are available from the literature,[36] and they are applicable to dilute electrolytic solutions. Available theoretical and empirical knowledge, however, is quite deficient in describing the transport properties of concentrated systems. The development of Onsager and Fuoss,[30] for example, accounts for the concentration dependence of diffusion coefficient in dilute electrolytic solutions but fails to predict large deviations from ideality in concentrated systems. The lack of accurate data for this important property at high concentrations is also a serious drawback in extending the analysis of mass transfer problems to concentrated solutions. This thesis is concerned with the correlation, prediction and measurement of diffusion coefficients in concentrated electrolytic solutions.

Several important works provided the background for discussions in the following chapters. The formulation of the flux equations and the definition of some transport properties, which offer a systematic treatment of mass transport in concentrated electrolytic solutions, are due to Newman.[28] His derivations consider the effect of the solvent flux, which is usually ignored in the treatments of dilute systems, and resolve the question of irreversiblity in concentrated solutions. We present a summary of these equations in Chapter II and put them in convenient forms for use in the chapters following.

In Chapter III we study the possibility of predicting diffusion coefficients in concentrated binary solutions from experimental viscosity and activity coefficient data. A compilation of the transport and thermodynamic properties of electrolytic solutions by Chapman and Newman [15] supply the necessary data. Chapman's results from the application of transport equations to available experimental data in his Ph.D. Thesis[7] provide a qualitative understanding of the behavior of various ionic species in aqueous solution. The works by Glasstone[16] and Podolsky[31] propose simple models on the microscopic nature of liquids and dilute electrolytic solutions. We modify these models for application to concentrated solutions and thereby propose a one parameter expression for the diffusion coefficient. We investigate the applicability of the regular solution assumptions in approximating the behavior of concentrated electrolytic solutions. In order to test our tentative models we compare our predicted values for the diffusion coefficient with experimental data on several electrolytic systems.

In our theoretical treatments we remain limited to systems with sufficient and accurate experimental data on viscosities, and diffusion coefficients. Our study is restricted due to the fact that most electrolytic systems lack viscosity data at low concentrations and diffusion coefficient data at high concentrations. We try to contribute in this respect by measuring the diffusion coefficient of nitric acid solutions over a wide concentration range. For this purpose we apply the results of restricted diffusion. We present and analyze the restricted diffusion model in Chapter IV following the original derivations by Chapman.[9]

In Chapter V we present our experimental method which utilizes Rayleigh interferometry for the measurement of concentration profiles in the course of diffusion. We report our experimental results on the

the diffusion coefficients and viscosities; the viscosity of nitric acid solutions are measured in dilute solutions with the purpose of complementing available data on this property. The results are finally correlated and evaluated with the aid of the equations presented in Chapter II. On the basis of these results we try to explain qualitatively the nature of ionic diffusion in aqueous nitric acid solutions.

II. A SURVEY OF THE FUNDAMENTALS OF MASS TRANSPORT IN CONCENTRATED ELECTROLYTIC SOLUTIONS

A method of formulating the equations of transport in concentrated solutions have been proposed by Newman, Bennion and Tobias[27] and discussed in detail in two other treatises.[28,5] The basic relationships will be presented here without much derivation, and the reader is directed to these references for more comprehensive treatment of the subject.

The transport equations in concentrated solutions comprise for each species i, a differential material balance

$$\frac{\partial c_i}{\partial t} = -\nabla \cdot \underline{N}_i + R_i, \tag{2-1}$$

a relation between the current density and the fluxes,

$$\underline{i} = F \sum_i z_i \underline{N}_i, \tag{2-2}$$

a condition of electroneutrality,

$$\Sigma \; z_i c_i = 0, \tag{2-3}$$

and a flux relation of the form,

$$c_i \nabla \mu_i = RT \sum_j \frac{c_i c_j}{c_{T,p} \mathcal{D}_{ij}} (\underline{v}_j - \underline{v}_i). \tag{2-4}$$

Equation (2-4) is, in a way, a force balance on species i. The left hand term can be regarded as a driving force per unit volume acting on species i. This force is counter-balanced by an opposite drag from the other components j and is proportional to the difference in the velocities of i and j.

The necessity of combining Eqs. (2-1) and (2-4) for more useful relationships requires explicit expressions for the fluxes. This can be

accomplished by inverting Eq. (2-4) with the utility of Eqs. (2-2) and (2-3). Thus, with respect to the solvent velocity and in the absence of current, the fluxes for salt and solvent in a binary solution become

$$\underline{N}_s = \frac{\underline{N}_+}{\nu_+} = \frac{\underline{N}_-}{\nu_-} = -\frac{c_{T,p}/c_o}{\nu\ RT}\ \mathfrak{D}_p c\ \nabla\mu_e + c\underline{v}_o, \qquad (2\text{-}5)$$

and

$$\underline{N}_o = c_o\ \underline{v}_o, \qquad (2\text{-}6)$$

where the diffusion coefficient is

$$\mathfrak{D}_p = \frac{\mathfrak{D}_{o+}\ \mathfrak{D}_{o-}\ (z_+ - z_-)}{z_+\ \mathfrak{D}_{o+} - z_-\ \mathfrak{D}_{o-}}, \qquad (2\text{-}7)$$

and

$$\mu_e = \nu_+\ \mu_+ + \nu_-\ \mu_- \qquad (2\text{-}8)$$

is the chemical potential of the electrolyte.

At constant temperature and pressure the gradient of the chemical potential is related to the activity of the salt as

$$\nabla\mu_e = RT\ \nabla \ln a_e = RT\left(\frac{\partial \ln a_e}{\partial c}\right)\nabla c. \qquad (2\text{-}9)$$

In terms of the activity coefficient on the molality scale this becomes

$$\nabla\mu_e = \nu RT\left(\frac{c_{T,p}^2}{c_o\ c}\right)\left(1 + \frac{d\ \ln\gamma}{d\ln m}\right)\frac{d\ (c/c_{T,p})}{dc}\ \nabla c, \qquad (2\text{-}10)$$

and further manipulation leads to the form,

$$\nabla\mu_e = \frac{\nu\ RT}{c\ c_o\ \bar{V}_o}\ \left(1 + \frac{d\ln\gamma}{d\ln m}\right)\ \nabla c, \qquad (2\text{-}11)$$

where $\bar{V}_o$ is the partial molar volume of the solvent, and m is the molality. Thus, Eq. (2-5) becomes

$$\underline{N}_s = -\frac{c_{T,p}}{c_o^2\ \bar{V}_o}\mathfrak{D}_p\ \left(1 + \frac{d\ln\gamma}{d\ln m}\right)\nabla c + c\underline{v}_o\ . \qquad (2\text{-}12)$$

An analogous expression is Fick's first law of diffusion, as stated by Bird, Stewart and Lightfoot,[3]

$$\underline{J}_s^* = c_{T,x}\ D\nabla x_s, \qquad (2\text{-}13)$$

where $\underline{J}_s^*$ is the molar flux of the salt relative for the molar average velocity $\underline{v}^*$ and is defined by,

$$\underline{J}_s^* = c\underline{v} - c\underline{v}^* = \underline{N}_s - (c/c_{T,x})(\underline{N}_s + c_o \underline{v}_o). \tag{2-14}$$

The concentration factor $c_{T,x}$ differs from $c_{T,p}$ such that

$$c_{T,x} = c + c_o, \tag{2-15}$$

and

$$c_{T,p} = \nu c + c_o. \tag{2-16}$$

The differential diffusion coefficient D is the quantity usually measured experimentally and reported in the literature. The mole fraction of the salt x_s is given by

$$x_s = c/c_{T,x}. \tag{2-17}$$

We can also define a "particle fraction" p_s as

$$p_s = c/c_{T,p}. \tag{2-18}$$

A flux expression analogous to Eq. (2-12) can now be derived from Eq. (2-13), using Eqs. (2-14) and (2-17) and noting that

$$\nabla x_s = \frac{\nabla c}{c_{T,x}^2 \bar{V}_o}. \tag{2-19}$$

Equation (2-13) can then be transformed into the form,

$$\underline{N}_s = - \frac{D\nabla c}{\bar{V}_o \; c_o} + c\underline{v}_o. \tag{2-20}$$

Comparison of Eqs. (2-12) and (2-20) yields

$$D = \frac{\mathfrak{D}_p}{p_o} \left(1 + \frac{d\ln\gamma}{d\ln m}\right), \tag{2-21}$$

where p_o is the particle fraction of the solvent.

Equation (2-21) is, in a sense, an alternative way of defining the thermodynamic diffusion coefficient $\mathfrak{D}_p$ in terms of parameters which

can be measured directly by experiment. Definition of the total solution concentration again brings us to a controversy because if we stick to the convention described by Eq. (2-15), we can define a different thermodynamic diffusion coefficient, such that

$$D = \frac{\mathcal{D}_x}{x_o} \left(1 + \frac{d\ln\gamma}{d\ln m}\right). \qquad (2\text{-}22)$$

Instead of adopting one of the conventions, we will use and compare both forms in the developments and discussion to be presented in Chapter III.

A useful transport property, the transference number with respect to the solvent velocity, can be related to the properties already defined namely,

$$t_+ = 1 - t_- = \frac{z_+ \mathcal{D}_{o+}}{z_+ \mathcal{D}_{o+} - z_- \mathcal{D}_{o-}}. \qquad (2\text{-}23)$$

Another transport equation to be mentioned is the relationship between the conductivity κ and the property $\mathcal{D}_{+-}$, given by

$$\frac{1}{\kappa} = \frac{-RT}{c_{T,p} z_+ z_- F^2} \left(\frac{1}{\mathcal{D}_{+-}} + \frac{c_o t_-}{c_+ \mathcal{D}_{o-}}\right). \qquad (2\text{-}24)$$

Equations (2-7), (2-21), (2-23), and (2-24) represent a convenient set of relationships to correlate the transport properties of electrolytic solutions. The number of unknown parameters in these equations, however, far exceed the number of equations themselves. One would require data on at least four of the properties to determine the remaining four. For the moment, at least, we can assume that two of the parameters, the activity coefficient and the conductivity are known. In fact, the activity coefficients and the conductivities appear to be the most abundant set of data available in the literature in comparison with the other transport properties. Newman et. al.[27] also offer a method for correlating the conductivities of electrolytes in dilute and concentrated

solutions. Their method is suitable for estimating conductivities in a wide range of concentrations given a few experimental data points. Redlich, Gargrave and Krostek[34] propose a method of similar utility for the correlation of activity coefficients. Thus, eliminating the activity coefficient and conductivity as unknowns, we are left with two unknowns to deal with. Robinson and Stokes[36,37] derive equations to predict transference numbers and correlate diffusivities, but these equations seem to be satisfactory for dilute solutions only. The theory on diffusion developed by Onsager and Fuoss[30] has the same drawback. A method for correlating diffusivities, proposed by Bhatia, Gubbins and Walker,[2] appears to be applicable to concentrated solutions, and it may be worth further consideration. Chapman[6] has made an attempt to predict $\mathfrak{D}_{+-}$; however, his method needs some improvement in order to obtain a more adequate description of this property. This feat is beyond the scope of this work. We will concentrate mainly on the correlation, prediction and measurement of diffusion coefficients as will be discussed in the following chapters.

III. METHODS OF CORRELATING AND PREDICTING DIFFUSIVITIES

In this chapter we present two methods to predict differential diffusion coefficients in concentrated electrolytic solutions from available experimental data on the viscosities and the activity coefficients. We attempt to correlate experimental diffusivity data by a one parameter equation, which also seems to be convenient for generating diffusivities over a wide range of concentrations from only a few experimental data points. Our discussion is therefore limited to a small number of electrolytic solutions for which sufficient and adequate data are available in the literature, concerning their viscosities, activity coefficients and diffusivities. We will also narrow the scope of our discussion to solutions at 25°C.

The methods involve some gross assumptions which may not be applicable to concentrated electrolyte solutions. Hence, each method is actually a tentative recommendation for the particular case to which it applies rather than a well developed theory, and the extent of agreement with the experimental foundings should determine its worth in applicability.

A. Predicting Diffusivities from Viscosity and Activity Coefficient Data

Experimental results on the non-electrolyte systems indicate that the thermodynamic diffusion coefficient, defined in an analogous fashion to $\mathfrak{D}_p$ and $\mathfrak{D}_x$ is less concentration dependent than the measured diffusion coefficient D, and furthermore, the product of the thermodynamic diffusion coefficient and the viscosity remain fairly constant over moderate ranges of concentration.[4] Newman, et al.[27] have assumed the same to hold true for electrolyte solutions in their conductivity correlation for potassium

chloride and potassium hydroxide. In order to test the validity of this assumption, we have calculated the values $\eta\mathcal{D}_p$ and $\eta\mathcal{D}_x$ for various electrolytic solutions. These values are given in Tables 3-1 through 3-9 and plotted in Figs. 3-1 through 3-9. The sources of diffusivity data are cited on each table. Viscosities and the activity coefficients were calculated from the correlation functions given in the Appendix.

The results can be explained by considering the effects of charged particles on the structure of water. Chapman's[7] results and discussion on the multicomponent diffusion coefficients $\mathcal{D}_{oi}$ of different ions in aqueous solution gives us clues about the behavior of the thermodynamic diffusion coefficient.

The shape of $\eta\mathcal{D}$ curves for ammonium chloride and the alkali halides indicate that the assumption is satisfactory for these electrolyte solutions with the exception of potassium iodide and lithium chloride. Chapman reports that the alkali metal ions smaller in size than potassium are structure making, and this ability increases with decreasing ionic size. Halogen ions, however, are structure breaking in proportion to their size. Behavior of the alkali metal ions generally dominate the behavior of the halogen ions in determining the effects of electrolyte on the structure of water. Sodium chloride, for example, improves the structure in solution due to the sodium ion, causing a drop in the diffusion coefficient and a simultaneous increase in the viscosity. The potassium halides and cesium chloride appear to be structure breaking since their multicomponent diffusion coefficients tend to increase at moderate concentrations. This effect can be attributed to relatively large sizes of the cations. At higher concentrations the multicomponent diffusion coefficients of these electrolytes decrease probably because

TABLE 3-1 Ammonium chloride in water at 25°C: Viscosity, thermodynamic diffusion coefficient, $\eta\mathfrak{D}$ values, experimental and calculated diffusion coefficients

EXP DATA ARE FROM HALL, WISHAW & STOKES, JACS 75, 1556 (1953)

c	η	D_{exp}	$\mathfrak{D}_p$	$\mathfrak{D}_x$
.100	.892	1.838	2.021	2.025
.200	.891	1.836	2.040	2.048
.300	.889	1.841	2.049	2.060
.500	.887	1.861	2.057	2.075
.700	.885	1.883	2.055	2.082
1.000	.883	1.921	2.049	2.087
1.500	.883	1.986	2.029	2.086
2.000	.885	2.051	2.003	2.079
2.500	.888	2.113	1.975	2.069
3.000	.894	2.164	1.940	2.052
3.250	.897	2.184	1.921	2.042
3.500	.901	2.203	1.904	2.034
4.000	.909	2.235	1.873	2.021
4.500	.918	2.257	1.850	2.016
5.000	.927	2.264	1.832	2.018

c	$\eta\mathfrak{D}_p$	$\eta\mathfrak{D}_x$	D_{cal} [a]	% Error [b]
.100	1.803	1.806	1.807	-1.707
.200	1.817	1.824	1.787	-2.656
.300	1.822	1.832	1.784	-3.080
.500	1.824	1.840	1.795	-3.544
.700	1.819	1.842	1.815	-3.635
1.000	1.810	1.843	1.850	-3.691
1.500	1.791	1.841	1.915	-3.577
2.000	1.772	1.839	1.980	-3.456
2.500	1.754	1.838	2.041	-3.404
3.000	1.734	1.835	2.094	-3.235
3.250	1.724	1.832	2.116	-3.103
3.500	1.715	1.832	2.135	-3.086
4.000	1.702	1.837	2.160	-3.345
4.500	1.697	1.850	2.166	-4.037
5.000	1.699	1.871	2.149	-5.098

[a] Calculated from Eq. (3-2)

[b] Percent error in the calculated diffusion coefficent = $(D_{cal} - D_{exp})/D_{exp}$

TABLE 3-2 Sodium chloride in water at 25°C: Viscosity, thermodynamic diffusion coefficient, $\eta\mathfrak{D}$ values, experimental and calculated diffusion coefficients

EXP DATA ARE FROM STOKES, JACS 72, 2243 (1950)

c	η	D_{exp}	$\mathfrak{D}_p$	$\mathfrak{D}_x$
-0.	.890	1.612	1.612	1.612
.050	.895	1.506	1.620	1.621
.100	.899	1.484	1.613	1.616
.200	.907	1.478	1.609	1.615
.300	.915	1.477	1.598	1.607
.500	.931	1.474	1.561	1.575
.700	.948	1.475	1.521	1.541
1.000	.975	1.483	1.464	1.491
1.500	1.026	1.495	1.363	1.400
2.000	1.084	1.514	1.269	1.315
2.500	1.150	1.529	1.174	1.227
3.000	1.225	1.544	1.083	1.143
3.500	1.310	1.559	.999	1.063
4.000	1.406	1.584	.928	.996

c	$\eta\mathfrak{D}_p$	$\eta\mathfrak{D}_x$	D_{cal} [a]	% Error [b]
-0.	1.435	1.435	1.612	-.000
.050	1.450	1.452	1.489	-1.136
.100	1.450	1.453	1.466	-1.236
.200	1.460	1.465	1.448	-2.054
.300	1.462	1.470	1.442	-2.376
.500	1.453	1.466	1.443	-2.135
.700	1.442	1.460	1.449	-1.734
1.000	1.428	1.454	1.464	-1.266
1.500	1.399	1.437	1.494	-.095
2.000	1.375	1.425	1.525	.714
2.500	1.349	1.411	1.556	1.733
3.000	1.327	1.399	1.584	2.561
3.500	1.309	1.393	1.607	3.057
4.000	1.306	1.401	1.622	2.425

[a,b] See footnotes on page 11.

TABLE 3-3 Potassium bromide in water at 25°C: Viscosity, thermodynamic diffusion coefficient, $\eta\mathfrak{D}$ values, experimental and calculated diffusion coefficients.

EXP DATA ARE FROM STOKES, JACS 72, 2243 (1950)

c	η	D_{exp}	$\mathfrak{D}_p$	$\mathfrak{D}_x$
-0.	.890	2.018	2.018	2.018
.050	.889	1.892	2.045	2.047
.100	.887	1.874	2.053	2.057
.200	.884	1.870	2.064	2.072
.300	.880	1.872	2.065	2.076
.500	.875	1.885	2.057	2.076
.700	.869	1.917	2.060	2.087
1.000	.863	1.975	2.065	2.103
1.500	.856	2.062	2.048	2.105
2.000	.854	2.132	2.002	2.077
2.500	.857	2.199	1.948	2.040
3.000	.864	2.280	1.904	2.013
3.500	.878	2.354	1.855	1.981
4.000	.896	2.434	1.817	1.959

c	$\eta\mathfrak{D}_p$	$\eta\mathfrak{D}_x$	D_{cal} [a]	% Error [b]
-0.	1.797	1.797	2.018	-.000
.050	1.818	1.819	1.868	-1.246
.100	1.821	1.824	1.845	-1.528
.200	1.824	1.831	1.835	-1.873
.300	1.818	1.828	1.840	-1.709
.500	1.799	1.816	1.865	-1.043
.700	1.791	1.814	1.899	-.949
1.000	1.782	1.815	1.955	-1.003
1.500	1.753	1.802	2.056	-.283
2.000	1.709	1.774	2.160	1.298
2.500	1.669	1.748	2.261	2.803
3.000	1.646	1.740	2.354	3.231
3.500	1.628	1.739	2.433	3.340
4.000	1.628	1.756	2.491	2.334

[a,b] See footnotes on page 11.

TABLE 3-4 Potassium chloride in water at 25°C: Viscosity, thermodynamic diffusion coefficient, $\eta\mathfrak{D}$ values, experimental and calculated diffusion coefficients.

EXP DATA ARE FROM GOSTING, JACS 72, 4418 (1950)

c	η	D_{exp}	$\mathfrak{D}_p$	$\mathfrak{D}_x$
.225	.890	1.838	2.041	2.049
.332	.889	1.840	2.042	2.054
.500	.889	1.850	2.040	2.059
1.000	.888	1.892	2.017	2.053
1.500	.890	1.943	1.977	2.032
2.000	.896	1.999	1.929	2.001
2.500	.906	2.057	1.875	1.962
3.001	.919	2.112	1.818	1.920
3.501	.938	2.160	1.762	1.878
3.901	.957	2.196	1.724	1.852
.100	.890	1.851	2.035	2.038

c	$\eta\mathfrak{D}_p$	$\eta\mathfrak{D}_x$	D_{cal} [a]	% Error [b]
.225	1.816	1.823	1.789	-2.675
.332	1.816	1.827	1.787	-2.888
.500	1.813	1.830	1.794	-3.029
1.000	1.791	1.824	1.841	-2.729
1.500	1.761	1.809	1.905	-1.924
2.000	1.729	1.793	1.979	-1.032
2.500	1.698	1.777	2.054	-.140
3.001	1.671	1.765	2.123	.515
3.501	1.653	1.762	2.175	.699
3.901	1.650	1.772	2.198	.126
.100	1.811	1.814	1.810	-2.204

[a,b] See footnotes on page 11.

TABLES 3-5 Cesium chloride in water at 25°C: Viscosity, thermodynamic diffusion coefficient, $\eta\mathfrak{D}$ values, experimental and calculated diffusion coefficients.

EXP DATA ARE FROM LYONS $ RILEY, JACS 76, 5216 (1954)

c	η	D_{exp}	$\mathfrak{D}_p$	$\mathfrak{D}_x$
.063	.882	1.887	2.091	2.093
.090	.881	1.874	2.101	2.105
.160	.879	1.859	2.123	2.129
.250	.877	1.855	2.143	2.153
.640	.868	1.868	2.165	2.190
1.000	.862	1.902	2.158	2.198
1.960	.851	2.023	2.093	2.171
3.060	.856	2.183	1.997	2.117
4.000	.880	2.291	1.895	2.048
5.000	.932	2.364	1.783	1.968
5.750	.993	2.354	1.679	1.884
6.000	1.018	2.335	1.639	1.850

c	$\eta\mathfrak{D}_p$	$\eta\mathfrak{D}_x$	D_{cal} [a]	% Error [b]
.063	1.845	1.847	1.859	-1.485
.090	1.852	1.855	1.839	-1.892
.160	1.866	1.871	1.808	-2.746
.250	1.879	1.887	1.789	-3.567
.640	1.880	1.902	1.787	-4.327
1.000	1.860	1.894	1.827	-3.928
1.960	1.780	1.847	1.993	-1.459
3.060	1.709	1.811	2.193	.464
4.000	1.669	1.803	2.313	.943
5.000	1.662	1.834	2.345	-.799
5.750	1.666	1.870	2.291	-2.697
6.000	1.668	1.883	2.257	-3.355

[a,b] See footnotes on page 11.

TABLE 3-6 Lithium chloride in water at 25°C: Viscosity, thermodynamic diffusion coefficient, $\eta\mathcal{D}$ values, experimental and calculated diffusion coefficients.

EXP DATA ARE FROM VITAGLIANO, GAZ CHIM ITAL 90, 876(1960)

c	η	D_{exp}	$\mathcal{D}_p$	$\mathcal{D}_x$
.117	.907	1.267	1.350	1.353
.128	.908	1.262	1.343	1.346
.168	.914	1.261	1.334	1.338
.272	.928	1.262	1.306	1.313
.316	.935	1.264	1.294	1.302
.335	.937	1.264	1.288	1.296
.422	.949	1.269	1.264	1.273
.587	.972	1.278	1.215	1.228
.660	.982	1.280	1.191	1.205
.944	1.021	1.300	1.112	1.131
1.164	1.052	1.317	1.055	1.077
1.666	1.125	1.346	.931	.959
1.898	1.160	1.346	.871	.901
2.049	1.184	1.370	.849	.881
2.833	1.316	1.417	.710	.747
3.206	1.386	1.436	.654	.692
3.811	1.512	1.461	.575	.615
4.091	1.576	1.469	.543	.583
4.454	1.665	1.473	.503	.543
4.634	1.712	1.474	.484	.525
5.933	2.120	1.455	.375	.416
6.386	2.298	1.438	.345	.385

c	$\eta\mathcal{D}_p$	$\eta\mathcal{D}_x$	D_{cal} [a]	% Error[b]
.117	1.224	1.226	1.257	-.823
.128	1.219	1.222	1.256	-.501
.168	1.219	1.223	1.254	-.533
.272	1.213	1.219	1.259	-.213
.316	1.210	1.216	1.264	-.029
.335	1.207	1.215	1.266	.134
.422	1.199	1.209	1.277	.626
.587	1.181	1.193	1.303	1.930
.660	1.170	1.183	1.315	2.761
.944	1.136	1.155	1.369	5.298
1.164	1.110	1.133	1.413	7.297
1.666	1.047	1.079	1.518	12.759
1.898	1.010	1.045	1.567	16.383
2.049	1.005	1.043	1.598	16.646
2.833	.935	.983	1.753	23.730
3.206	.907	.960	1.819	26.686
3.811	.870	.930	1.910	30.753
4.091	.855	.919	1.944	32.365
4.454	.837	.905	1.980	34.421
4.634	.829	.899	1.994	35.264
5.933	.795	.881	2.008	38.033
6.386	.792	.885	1.977	37.479

[a,b] See footnotes on page 11.

TABLE 3-7 Potassium iodide in water at 25°C: Viscosity, thermodynamic diffusion coefficient, $\eta\mathfrak{D}$ values, experimental and calculated diffusion coefficients.

EXP DATA ARE FROM DUNLOF $ STOKES, JACS 73, 5456 (1951)

c	η	D_{exp}	$\mathfrak{D}_p$	$\mathfrak{D}_x$
-0.	.890	2.001	2.001	2.001
.050	.886	1.891	2.033	2.035
.100	.883	1.865	2.029	2.033
.200	.876	1.859	2.037	2.044
.300	.869	1.884	2.064	2.076
.500	.857	1.955	2.132	2.152
.700	.847	2.001	2.169	2.197
1.000	.834	2.065	2.217	2.258
1.500	.817	2.166	2.296	2.361
2.000	.808	2.254	2.377	2.469
2.500	.806	2.347	2.493	2.615
3.000	.811	2.440	2.657	2.816
3.500	.822	2.533	2.897	3.101

c	$\eta\mathfrak{D}_p$	$\eta\mathfrak{D}_x$	D_{cal} [a]	% Error [b]
-0.	1.781	1.781	2.001	-.000
.050	1.802	1.804	1.868	-1.232
.100	1.791	1.794	1.852	-.706
.200	1.783	1.790	1.850	-.469
.300	1.795	1.804	1.860	-1.269
.500	1.828	1.845	1.888	-3.449
.700	1.837	1.860	1.916	-4.245
1.000	1.848	1.882	1.954	-5.359
1.500	1.877	1.930	1.999	-7.701
2.000	1.922	1.996	2.012	-10.729
2.500	2.010	2.108	1.983	-15.488
3.000	2.154	2.283	1.904	-21.956
3.500	2.382	2.550	1.770	-30.141

[a,b] See footnotes on page 11.

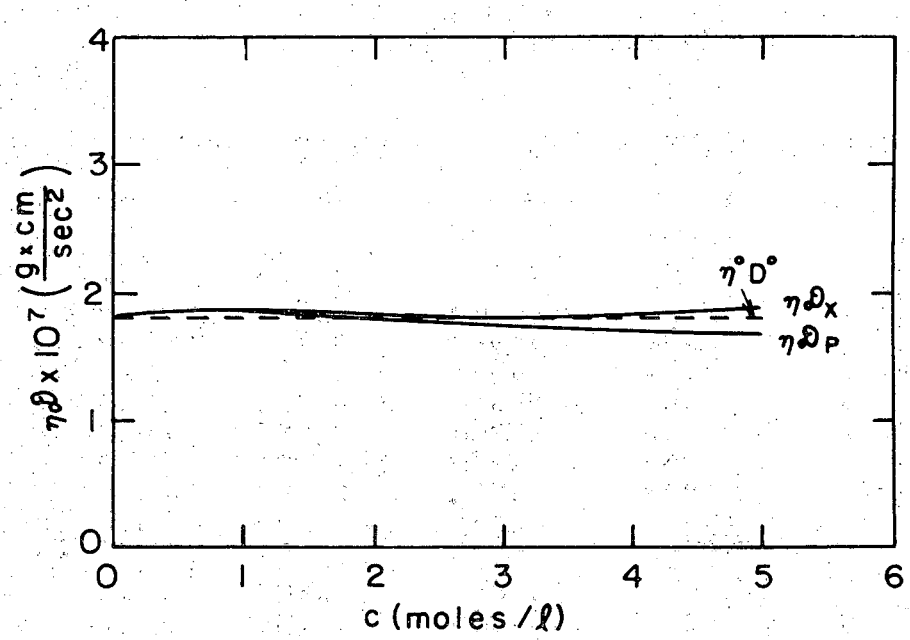

Fig. 3-1 $\eta\mathcal{D}$ curves of ammonium chloride in water at 25°C

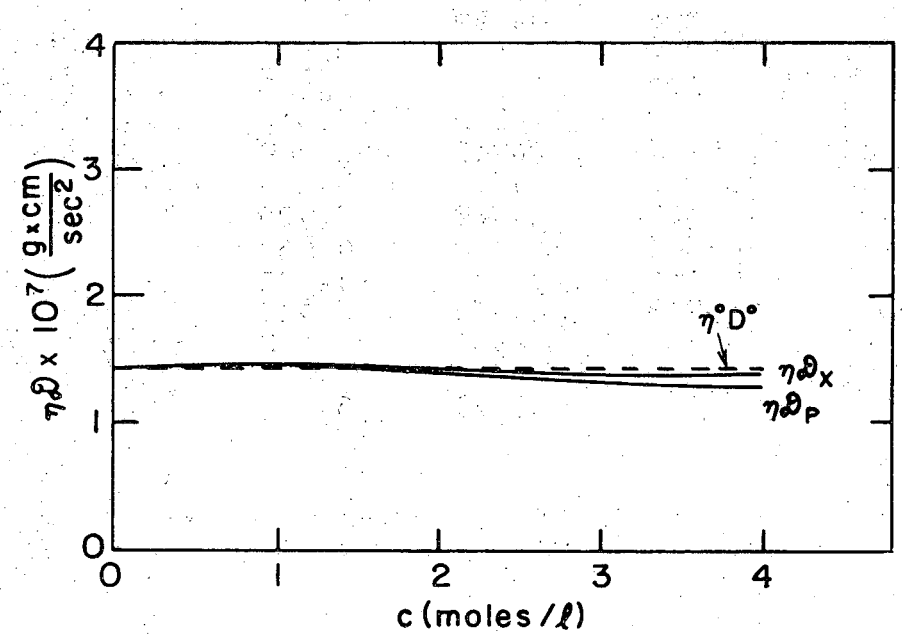

XBL 6911-6579

Fig. 3-2 $\eta\mathcal{D}$ curves of sodium chloride in water at 25°C.

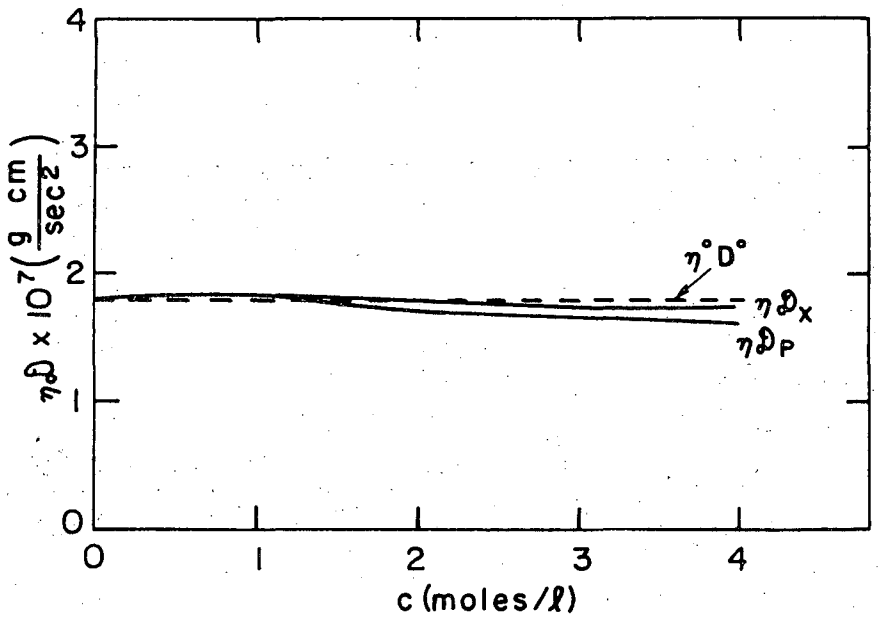

Fig. 3-3 $\eta\mathcal{D}$ curves of potassium bromide in water at 25°C

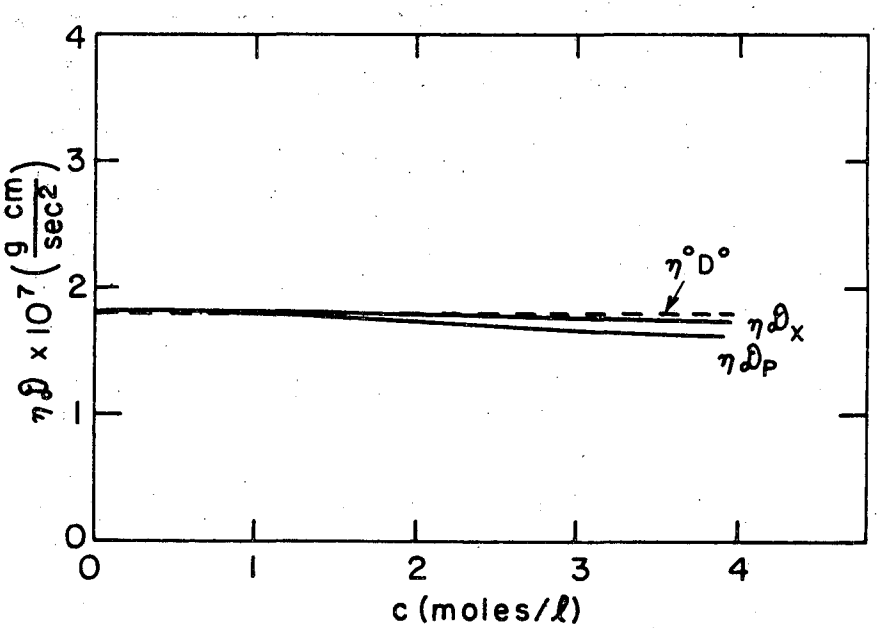

XBL 6911-6582

Fig. 3-4 $\eta\mathcal{D}$ curves of potassium chloride in water at 25°C

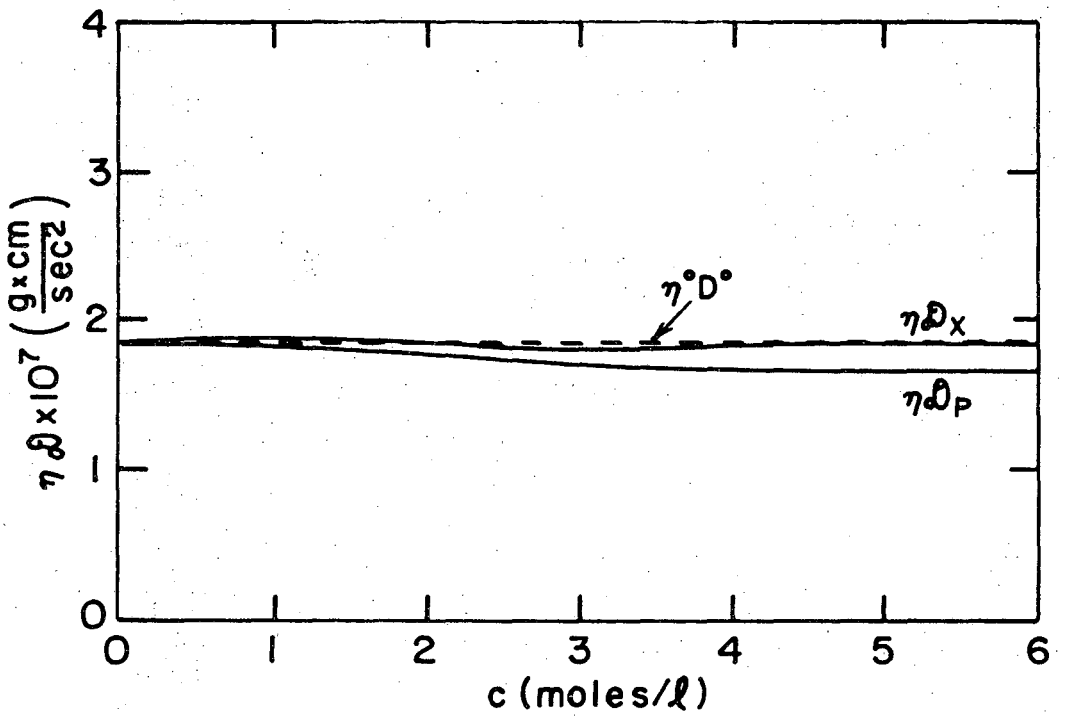

XBL 6911-6583

Fig. 3-5 $\eta\mathcal{D}$ curves of cesium chloride in water at 25°C

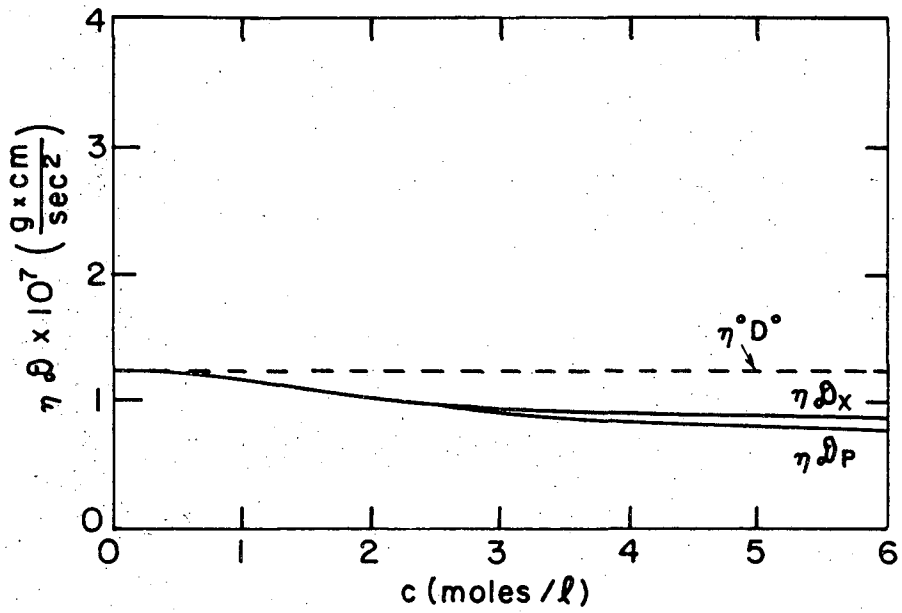

Fig. 3-6 $\eta\mathcal{D}$ curves of lithium chloride in water at 25°C.

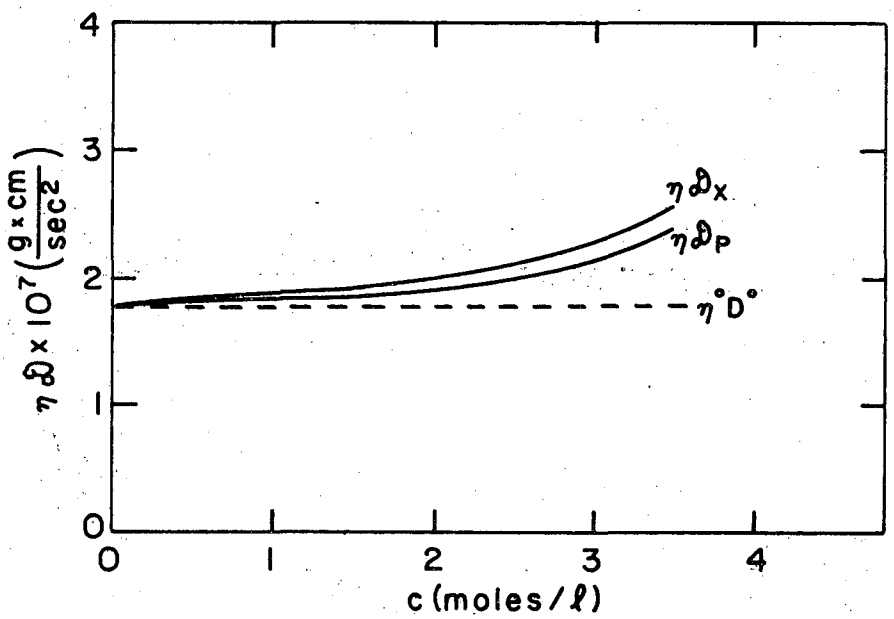

XBL 6911-6584

Fig. 3-7 $\eta\mathcal{D}$ curves of potassium iodide in water at 25°C.

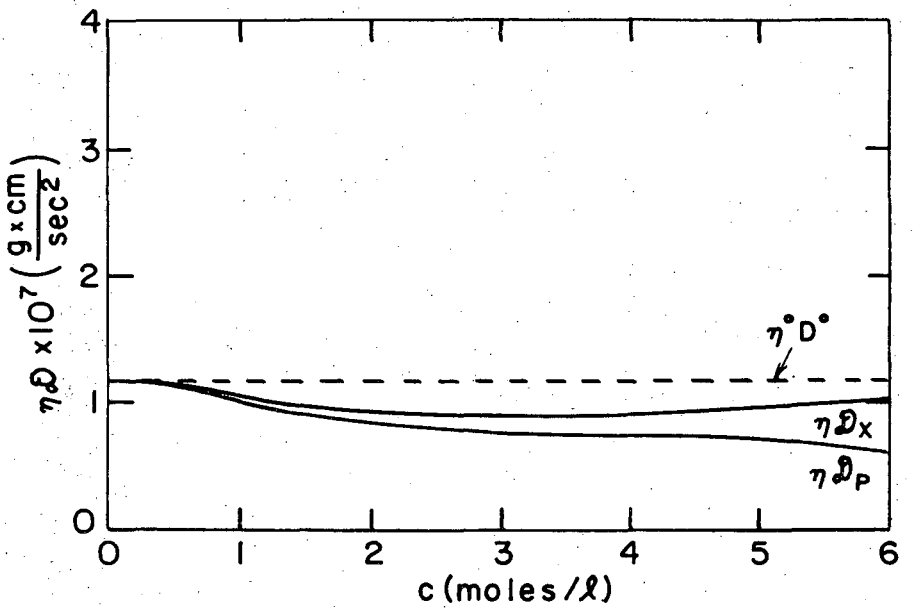

Fig. 3-8 $\eta\mathcal{D}$ curves of calcium chloride in water at 25°C.

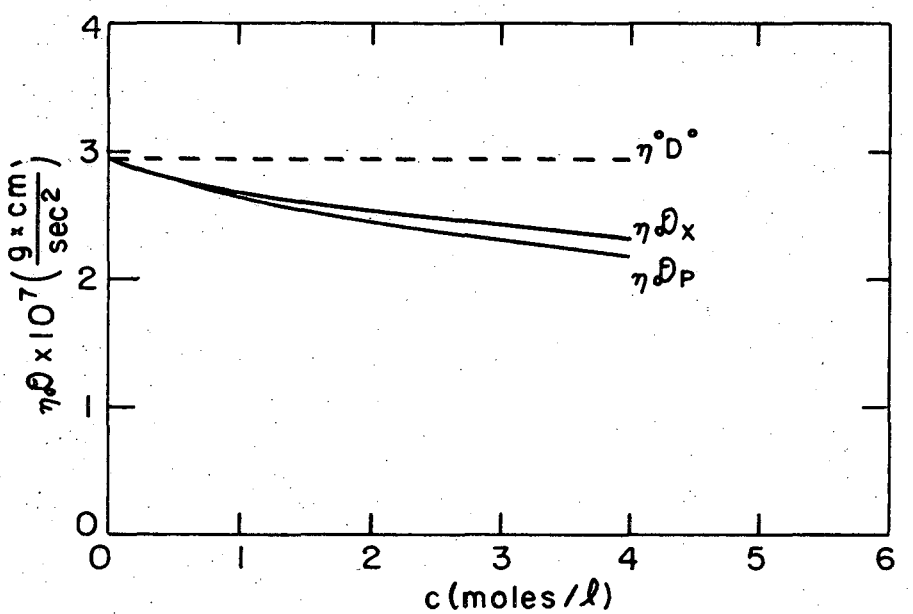

XBL 6911-6585

Fig. 3-9 $\eta\mathcal{D}$ curves of hydrochloric acid in water at 25°C.

of ionic association. Large ions tend to associate faster in comparison to small ions with increasing concentration.[32] The thermodynamic diffusion coefficient exhibits similar changes. In contrast the viscosities decrease to a shallow minimum and then increase at higher concentrations. Opposing behaviors of the thermodynamic diffusion coefficient and the viscosity in NaCl, KBr, KCl and CsCl solutions seem to compensate so as to keep the product $\eta\mathcal{D}$ fairly constant and roughly equal to the value at infinite dilution, $\eta^{\circ}D^{c}$, over a large concentration range.

Ammonium chloride has a striking similarity to KCl as far as its thermodynamic and transport properties are concerned. Hence, both electrolytes appear to show similar effects on the structure of water and can therefore be grouped in the same category.

Potassium iodide behaves in a similar way to KCl and KBr, but the structure breaking effect is more pronounced due to the large size of the iodide ion. This effect and high viscosities in the concentrated solution cause a positive deviation in the $\eta\mathcal{D}$ curves.

The lithium ion, due to its high charge relative to its size, is strongly structure making. As a result, the lithium salts exhibit relatively low diffusion coefficients in aqueous solution. This explains the negative deviations in $\eta\mathcal{D}$ for LiCl. The acid solutions act in a similar manner to the lithium salts.

The only polyvalent electrolyte studied was $CaCl_2$ because experimental data are even more scarce for such electrolytes at high concentrations. The calcium ion is believed to be structure making because of its high positive charge. The negative deviation of the $\eta\mathcal{D}_x$ curve up to moderate concentrations supports this hypothesis. The curve exhibits a minimum at moderate concentrations and then increases with the degree of association in solution.

An apparent feature of the $\eta\mathfrak{D}$ curves is that $\eta\mathfrak{D}_p$ values fall invariably below the values for $\eta\mathfrak{D}_x$. This observation is attributed to the fact that the particle fraction is always smaller than the mole fraction for any given concentration except at infinite dilution. For alkali chlorides and bromides, $\eta\mathfrak{D}_p$ always deviates slightly below its limiting value due to the dominating structure making effect of the alkali metal ion. For these cases it seems to be convenient to choose $\mathfrak{D}_x$ to predict the differential diffusion coefficients because $\eta\mathfrak{D}_x$ curves show smaller deviations compared to the $\eta\mathfrak{D}_p$ curves. In some cases these deviations are almost non-existent. Furthermore, in studying the behavior of electrolytes in aqueous solution based on such plots, the $\eta\mathfrak{D}_x$ curves seem to be more reliable because the $\eta\mathfrak{D}_p$ values fail to show the effects of ionic association such as in calcium chloride. This is caused by the fact that the calculation of $\mathfrak{D}_p$ is based on complete dissociation of the electrolyte. $\mathfrak{D}_x$ values do not necessarily carry such an assumption since they are defined in terms of the mole fraction of solute.

We have calculated the diffusion coefficients of various electrolytes following the assumption that the product $\eta\mathfrak{D}_x$ is constant and equal to the limiting value $\eta^\circ D^\circ$. In mathematical terms this can be expressed as

$$\eta\mathfrak{D}_x = \eta^\circ D^\circ. \qquad (3\text{-}1)$$

Combining this with Eq. (2-22) we obtain an expression for the diffusion coefficient,

$$D = \frac{\eta^\circ D^\circ}{\eta x_o}\left(1 + \frac{d\ln\gamma}{d\ln m}\right). \qquad (3\text{-}2)$$

Equation (3-2) conforms with the results obtained by Hartley and Crank.[20] Their discussion and Eq. (3-2) imply the regular solution assumption as has been shown by Bearman.[1] The results of our calculations are given in tables of previous pages and plotted in Figs. 3-12 through

3-16 for NH_4Cl, NaCl, KCl, KBr and CsCl. For these electrolytes the calculated diffusivities deviate from the experimental data at the most by 5%.

Another method will be recommended in Section C as an extention of the developments in this section and in Section B in order to predict the diffusion coefficients of electrolyte solutions, which do not follow the assumption of Eq. (3-1).

B. Development of a One Parameter Equation for the Diffusion Coefficient

Glasstone, Laidler and Eyring[16] propose a rate equation for diffusion in dilute, ideal solutions based on the absolute reaction rate theory. Following their discussion, we can write Fick's first law of diffusion in the z direction as

$$N_s = -D \frac{dc}{dz} . \tag{3-3}$$

This equation applies for dilute solutions only.

In order to diffuse in solution, a molecule of solute and one of solvent are required to slip past each other. Suppose the distance between two successive equilibrium positions is λ, so that this is the distance through which a molecule of solute is transported in each jump. The concentrations of solute in initial and final states of diffusion are then c and $c + \lambda\,(dc/dz)$ respectively. The flux of molecules moving in the forward direction is given by

$$N_{s,f} = c\,\lambda\,k, \tag{3-4}$$

where k is the specific reaction rate for diffusion, i.e., the number of times a molecule moves from one position to the next per unit time. Similarly, the rate of movement, in the backward direction is,

$$N_{s,b} = (c + \lambda\,(dc/dz))\,\lambda\,k. \tag{3-5}$$

The resultant flow in the forward direction is then

$$N_s = -\lambda^2 k (dc/dz). \tag{3-6}$$

Combining Eqs. (3-3) and (3-6), one obtains

$$D = \lambda^2 k . \tag{3-7}$$

According to the theory of absolute reaction rates,[17] the specific rate constant can be written as

$$k = \frac{kT}{h} e^{-\Delta F_o^*/RT}, \tag{3-8}$$

where ΔF_o^* is the activation free energy of transition. Thus, Eq. (3-7) becomes

$$D = k_D \lambda^2 e^{-\Delta F_o^*/RT}, \tag{3-9}$$

where

$$k_D = \frac{kT}{h} .$$

Podolsky[31] extends this theory to dilute electrolyte solutions in terms of a lattice model for diffusion in liquids. A solution corresponds to a lattice with particles of several species distributed among the sites. We make the assumption that Eq. (3-9), which was derived for lattice particles characterized by a single activation energy, can be generalized for electrolytic solutions if ΔF_o^* is taken as the average activation energy of the particles that are subject to a directional bias generated by the concentration gradient. Equation (3-9) does not suggest such a bias for any diffusing particle because it is an expression for the mutual diffusion coefficient. However, if we assume that the partial molal volumes of solute and solvent are constant, the mutual diffusion coefficient will be the same as the self-diffusion coefficient of water on the fixed volume reference frame.[20] In that case, the solvent molecules can be considered as being subject to the

directional bias. The free energy term in Eq. (3-9) should therefore refer to the solvent, and in an electrolytic solution this term can be written in the form,

$$\Delta F_o^* = \overline{\Delta F}_o^* + n_+ \delta_+ + n_- \delta_- . \qquad (3\text{-}10)$$

Equation (3-10) represents the perturbations in the average activation energies of water molecules due to interactions with the ions of solute. $\overline{\Delta F}_o^*$ is the average activation energy of the unperturbed water molecules, n_i is the number of particles of species i that interact with a single solvent molecule, and δ_i is the perturbation of the activation energy of water, caused by a single particle of species i. In terms of the particle fraction, n_i is given by

$$n_i = np_i = n\,\nu_i p, \qquad (3\text{-}11)$$

where n is the total number of particles, including the solvent molecules, that interact with a molecule of water.

Combining Eqs. (3-9), (3-10) and (3-11) we obtain for the diffusion coefficient,

$$D = k_D \lambda^2 \exp\left\{-\frac{np}{RT}(\nu_+ \delta_+ + \nu_- \delta_-)\right\} . \qquad (3\text{-}12)$$

Equations of a similar form have also been discussed by various authors[2,33,18] We extend Eq. (3-12) to concentrated solutions by writing

$$D = k_D \lambda^2 \left(\frac{d\ln a_e}{d\ln p}\right) \exp\left\{-\frac{np}{RT}(\nu_+ \delta_+ + \nu_- \delta_-)\right\}, \qquad (3\text{-}13)$$

where a_e is the activity of solute. Equation (3-13) can be transformed into the form,

$$D = \frac{D^o}{p_o}\left(1 + \frac{d\ln\gamma}{d\ln m}\right) \exp\left\{-\frac{np}{RT}(\nu_+ \delta_+ + \nu_- \delta_-)\right\} . \qquad (3\text{-}14)$$

Comparing this with Eq. (2-21), we obtain

$$\frac{\mathcal{D}_p}{D^o} = \exp\left\{-\frac{np}{RT}(\nu_+ \delta_+ + \nu_- \delta_-)\right\} . \qquad (3\text{-}15)$$

We wish to modify this equation in order to account for the electrophoretic effect. Furthermore, we note that the terms inside the exponential bracket are constant for a given electrolyte at a fixed temperature, except for the particle fraction. We therefore write

$$\frac{\mathcal{D}_p}{D^o + \Delta_1 + \Delta_2} = e^{qp}, \tag{3-16}$$

where q is a constant, and Δ_1, Δ_2 are the electrophoretic correction terms.

The electropohretic effect is caused when an ion moves through a viscous medium and tends to drag along with it the solution in its vicinity. Expressions for the electrophoretic terms are

$$\Delta_1 = \frac{kT}{6\pi\eta} \frac{(z_+ t_-^o + z_- t_+^o)^2}{z_+ z_-} \frac{K}{1+Ka} \tag{3-17}$$

for both symmetrical and unsymmetrical electrolytes, and

$$\Delta_2 = \frac{e^2}{12\pi\eta\epsilon} \left(\frac{|z|}{a}\right)^2 (Ka)^2 \left(\frac{e^{Ka}}{1+Ka}\right)^2 \int_a^\infty \frac{e^{-2Kr}}{r} dr, \tag{3-18}$$

for symmetrical electrolytes only. K is given by,

$$K = 0.5e \left(\frac{\pi N_{Avo}}{10\epsilon kT}\right)^{1/2} (c_+ z_+^2 + c_- z_-^2)^{1/2}. \tag{3-19}$$

The constant a is the ion size parameter and ϵ is the dielectric constant of solvent. The integral in Eq. (3-18) can be found tabulated as an exponential integral function[24] or calculated numerically on a digital computer. The second electrophoretic term does not apply to non-symmetrical electrolytes; its value, therefore, should be taken as zero for such cases.[38] A detailed discussion of the electrophoretic effect can be found in References 38 and 40.

The form of Eq. (3-16) suggests that a plot of $\ln[\mathcal{D}_p/(D^o+\Delta_1+\Delta_2)]$ versus p should yield a straight line of slope q. Such plots for several

electrolytes are shown in Figs. (3-10) and (3-11). In calculating the electrophoretic terms, we have used ion size parameters given in Robinson and Stokes[39] and tabulated in Table (3-10). Transference numbers and diffusion coefficients at infinite dilution were obtained from tables in Chapman's Ph.D. thesis.[8] The data were fit to straight lines and the slopes calculated by the method of least squares. The fit is better at higher concentrations. Knowing the slope, q, diffusivities can be calculated from

$$D = \frac{D^o+\Delta_1+\Delta_2}{p_o} \left(1 + \frac{d\ln\gamma}{d\ln m}\right) e^{qp}. \qquad (3\text{-}20)$$

Replacing the activity factor in Eq. (3-13) by (dlna/dlnx) would lead to the derivation of analogous equations in terms of $\mathcal{D}_x$ and the mole fraction. If we follow this convention, Eqs. (3-16) and (3-20) will read

$$\frac{\mathcal{D}_x}{D^o+\Delta_1+\Delta_2} = e^{q'p}, \qquad (3\text{-}21)$$

and

$$D = \frac{D^o+\Delta_1+\Delta_2}{x_o} \left(1 + \frac{d\ln\gamma}{d\ln m}\right) e^{q'p}. \qquad (3\text{-}22)$$

At this point where we are trying to correlate available diffusivity data, it seems not to make much difference whether we use one or the other convention. Equation (3-20) appears to give slightly better results. Diffusion coefficients, calculated from Eqs. (3-20) and (3-22) are given in Tables 3-11 through 3-18 for comparison. The results obtained from Eq. (3-20) are plotted in Figs. 3-12 through 3-15 and 3-19 through 3-22. Error in the calculated values is at the worst 3% for all uni-univalent electrolytes studied. Error in the calculated diffusivity of $CaCl_2$ goes up to 15% at one point.

The convenience of this correlation method is that when experimental diffusivity data are fitted to the logarithm of Eq. (3-16), one

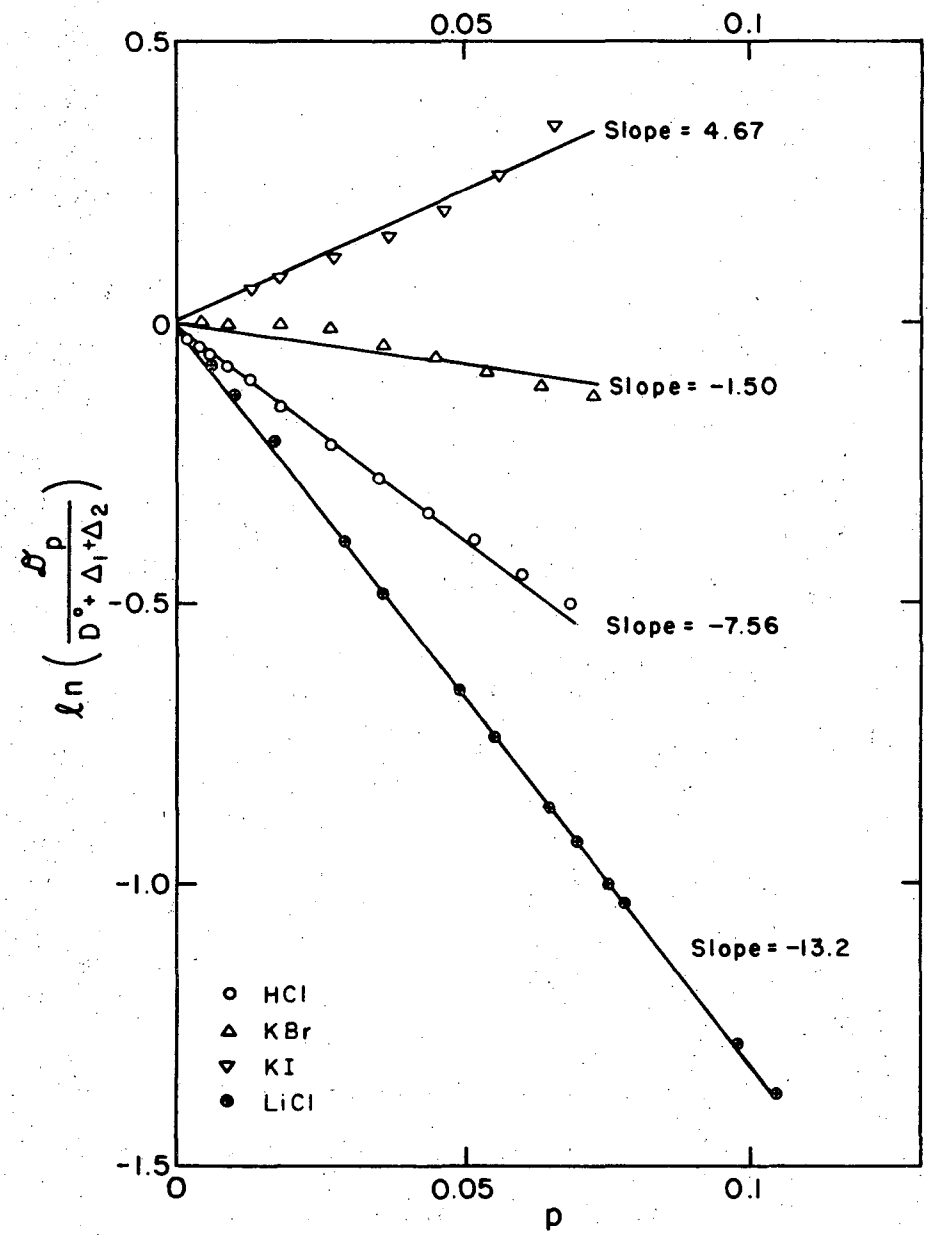

XBL 6912-6674

Fig 3-10 Diffusivity correlation for selected electrolytic solutions at 25°C.

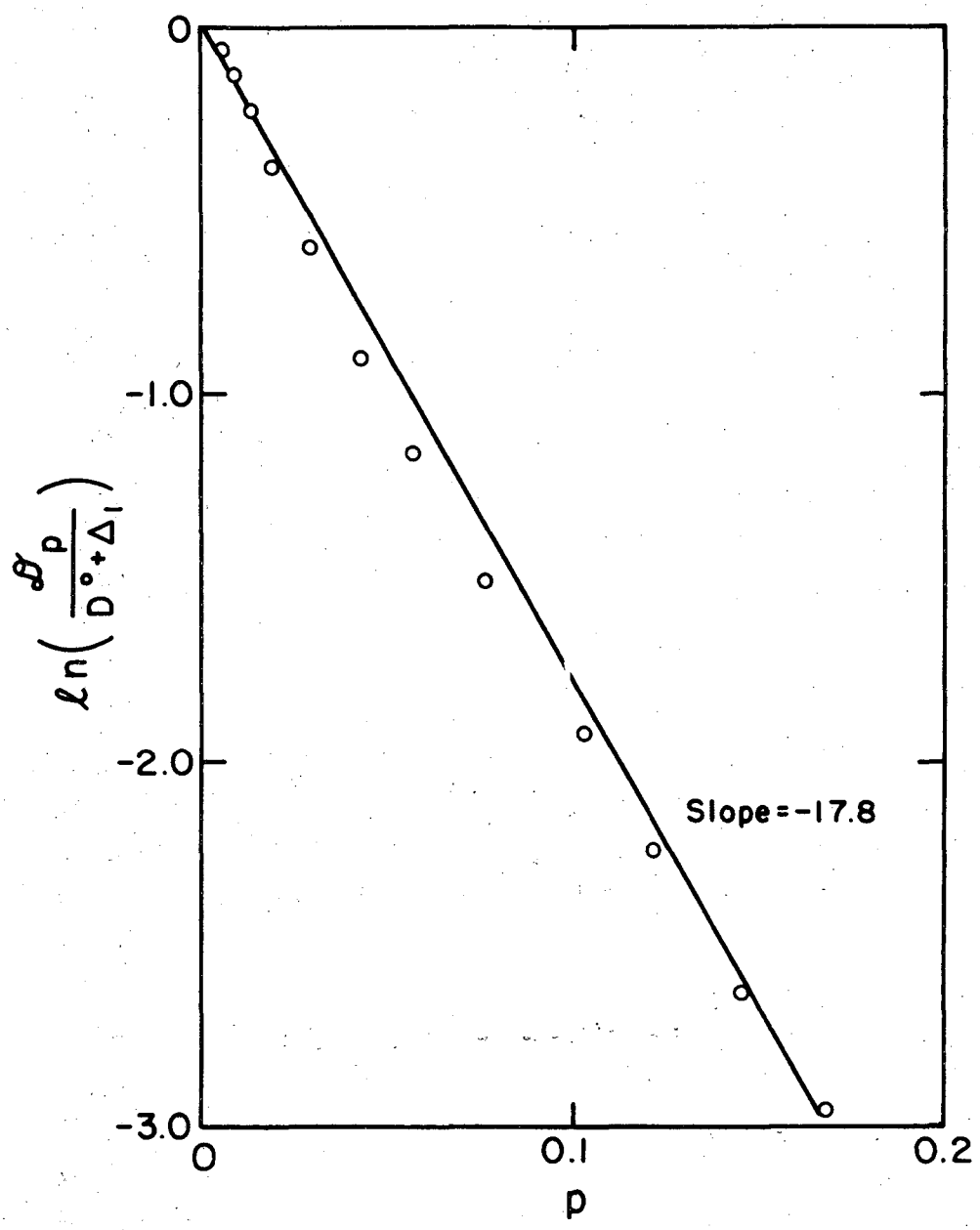

XBL 6911-6580

Fig. 3-11 Diffusivity correlation for calcium chloride in water at 25°C.

TABLES 3-10. Ion size parameters of selected electrolytes in aqueous solution at 25°C.

Solute	a (Angstrom)
HCl	4.47
LiCl	4.32
NaCl	3.97
KCl	3.63
KBr	3.85
KI	4.16
NH_4Cl	3.75
$CaCl_2$	4.73

TABLE 3-11 Experimental and calculated diffusion coefficients of ammonium chloride in water at 25°C.

EXP DATA ARE FROM HALL, WISHAW $ STOKES, JACS 75, 1556 (1953)

c	D_{exp}	D_{cal} [d]	% Error	D_{cal} [e]	% Error
.100	1.838	1.841	.157	1.841	.163
.200	1.836	1.827	-.511	1.827	-.498
.300	1.841	1.825	-.869	1.825	-.851
.500	1.861	1.835	-1.398	1.836	-1.369
.700	1.883	1.853	-1.614	1.853	-1.575
1.000	1.921	1.886	-1.836	1.887	-1.787
1.500	1.986	1.950	-1.823	1.951	-1.761
2.000	2.051	2.019	-1.570	2.020	-1.504
2.500	2.113	2.088	-1.177	2.089	-1.115
3.000	2.164	2.154	-.482	2.155	-.435
3.250	2.184	2.183	-.026	2.184	.011
3.500	2.203	2.211	.348	2.211	.372
4.000	2.235	2.255	.886	2.255	.876
4.500	2.257	2.281	1.076	2.280	1.022
5.000	2.264	2.286	.956	2.283	.847

[d] Calculated from Eq. (3-20)

[e] Calculated from Eq. (3-22)

TABLE 3-12 Experimental and calculated diffusion coefficients of sodium chloride in water at 25°C.

EXP DATA ARE FROM STOKES, JACS 72, 2243 (1950)

c	D_{exp}	D_{cal} [d]	% Error	D_{cal} [c]	% Error
-0.	1.612	1.612	0.	1.612	0.
.050	1.506	1.505	-.094	1.505	-.091
.100	1.484	1.484	.016	1.484	.021
.200	1.478	1.466	-.830	1.466	-.821
.300	1.477	1.457	-1.369	1.457	-1.355
.500	1.474	1.449	-1.710	1.449	-1.690
.700	1.475	1.447	-1.925	1.447	-1.898
1.000	1.483	1.449	-2.298	1.449	-2.265
1.500	1.495	1.462	-2.193	1.463	-2.156
2.000	1.514	1.484	-1.964	1.485	-1.930
2.500	1.529	1.513	-1.040	1.513	-1.017
3.000	1.544	1.547	.191	1.547	.197
3.500	1.559	1.584	1.596	1.584	1.576
4.000	1.584	1.622	2.379	1.621	2.325

[d,e] See footnotes on page 35.

TABLE 3-13 Experimental and calculated diffusion coefficients of potassium bromide in water at 25°C.

EXP DATA ARE FROM STOKES, JACS 72, 2243 (1950)

c	D_{exp}	D_{cal} [d]	% Error	D_{cal} [e]	% Error
-0.	2.018	2.018	0.	2.018	0.
.050	1.892	1.887	-.256	1.887	-.254
.100	1.874	1.867	-.354	1.867	-.349
.200	1.870	1.856	-.741	1.856	-.731
.300	1.872	1.857	-.805	1.857	-.790
.500	1.885	1.871	-.760	1.871	-.737
.700	1.917	1.891	-1.334	1.892	-1.305
1.000	1.975	1.929	-2.317	1.930	-2.281
1.500	2.062	2.004	-2.808	2.005	-2.766
2.000	2.132	2.090	-1.955	2.091	-1.915
2.500	2.199	2.185	-.628	2.186	-.599
3.000	2.280	2.285	.240	2.286	.249
3.500	2.354	2.387	1.403	2.387	1.381
4.000	2.434	2.485	2.082	2.483	2.019

[d,e] See footnote on page 35.

TABLE 3-14 Experimental and calculated diffusion coefficients of potassium chloride in water at 25°C.

EXP DATA ARE FROM GOSTING, JACS 72, 4418 (1950)

c	D_{exp}	D_{cal} [d]	% Error	D_{cal} [e]	% Error
.225	1.838	1.821	-.910	1.822	-.899
.332	1.840	1.819	-1.157	1.819	-1.141
.500	1.850	1.822	-1.513	1.822	-1.492
1.000	1.892	1.852	-2.127	1.853	-2.093
1.500	1.943	1.902	-2.116	1.902	-2.076
2.000	1.999	1.966	-1.690	1.966	-1.653
2.500	2.057	2.039	-.851	2.040	-.825
3.001	2.112	2.117	.217	2.117	.224
3.501	2.160	2.189	1.321	2.188	1.299
3.901	2.196	2.236	1.860	2.235	1.807
.100	1.851	1.838	-.687	1.839	-.682

[d,e] See footnotes, on page 35.

TABLE 3-15 Experimental and calculated diffusion coefficients of calcium chloride in water at 25°C.

EXP DATA ARE FROM LYONS & RILEY, JACS 76, 5216 (1954)

c	D_{exp}	D_{cal} [d]	% Error	D_{cal} [e]	% Error
.028	1.153	1.131	-1.915	1.131	-1.895
.055	1.136	1.095	-3.624	1.095	-3.586
.102	1.122	1.070	-4.659	1.071	-4.588
.193	1.123	1.064	-5.295	1.065	-5.162
.314	1.132	1.082	-4.438	1.084	-4.220
.469	1.152	1.119	-2.843	1.123	-2.513
.671	1.177	1.175	-.133	1.181	.348
1.000	1.220	1.270	4.058	1.279	4.796
1.442	1.271	1.383	8.800	1.397	9.889
1.462	1.271	1.387	9.158	1.401	10.264
2.046	1.310	1.488	13.615	1.509	15.159
2.570	1.311	1.513	15.386	1.537	17.245
3.250	1.248	1.430	14.568	1.456	16.637
4.001	1.078	1.191	10.472	1.211	12.370
4.486	.919	.978	6.414	.991	7.876
5.012	.716	.729	1.802	.733	2.383
5.424	.571	.544	-4.770	.541	-5.295
6.004	.402	.329	-18.238	.318	-20.992

[d,e] See footnotes on page 35.

TABLE 3-16 Experimental and calculated diffusion coefficients of hydrochloric acid in water at 25°C.

EXP DATA ARE FROM STOKES, JACS 72, 2243 (1950)

c	D_{exp}	D_{cal} [d]	% Error	D_{cal} [e]	% Error
-0.	3.339	3.339	0.	3.339	0.
.050	3.073	3.084	.344	3.084	.347
.100	3.050	3.057	.237	3.057	.241
.200	3.064	3.067	.102	3.067	.111
.300	3.093	3.104	.354	3.104	.368
.500	3.184	3.204	.625	3.205	.646
.700	3.286	3.317	.941	3.318	.968
1.000	3.436	3.494	1.697	3.495	1.731
1.500	3.743	3.793	1.343	3.795	1.381
2.000	4.046	4.086	.995	4.088	1.030
2.500	4.337	4.368	.710	4.369	.734
3.000	4.658	4.634	-.509	4.635	-.504
3.500	4.920	4.883	-.759	4.882	-.779
4.000	5.170	5.110	-1.156	5.108	-1.207

[d,e] See footnotes on page 35.

TABLE 3-17 Experimental and calculated diffusion coefficients of potassium iodide in water at 25°C.

EXP DATA ARE FROM DUNLOF $ STOKES, JACS 73, 5456 (1951)

c	D_{exp}	D_{cal} [d]	% Error	D_{cal} [e]	% Error
-0.	2.001	2.001	0.	2.001	0.
.050	1.891	1.890	-.059	1.890	-.056
.100	1.865	1.883	.954	1.883	.959
.200	1.859	1.893	1.819	1.893	1.829
.300	1.884	1.912	1.484	1.912	1.498
.500	1.955	1.957	.120	1.958	.140
.700	2.001	2.005	.218	2.006	.244
1.000	2.065	2.078	.645	2.079	.677
1.500	2.166	2.198	1.475	2.199	1.511
2.000	2.254	2.308	2.381	2.308	2.412
2.500	2.347	2.395	2.039	2.395	2.053
3.000	2.440	2.443	.130	2.443	.118
3.500	2.533	2.435	-3.866	2.434	-3.913

TABLE 3-18 Experimental and calculated diffusion coefficients of lithium chloride in water at 25°C

EXP DATA ARE FROM VITAGLIANO, GAZ CHIM ITAL 90, 876(1960)

c	D_{exp}	D_{cal} [d]	% Error	D_{cal} [e]	% Error
.117	1.267	1.257	-.805	1.257	-.797
.128	1.262	1.255	-.528	1.255	-.518
.168	1.261	1.252	-.748	1.252	-.736
.272	1.262	1.249	-1.050	1.249	-1.031
.316	1.264	1.249	-1.163	1.250	-1.142
.335	1.264	1.250	-1.130	1.250	-1.107
.422	1.269	1.253	-1.269	1.253	-1.241
.587	1.278	1.262	-1.241	1.263	-1.203
.660	1.280	1.267	-1.009	1.268	-.968
.944	1.300	1.289	-.871	1.289	-.816
1.164	1.317	1.307	-.788	1.307	-.724
1.666	1.346	1.348	.132	1.349	.210
1.898	1.346	1.366	1.491	1.367	1.574
2.049	1.370	1.378	.551	1.379	.634
2.833	1.417	1.429	.873	1.431	.953
3.206	1.436	1.448	.869	1.450	.941
3.811	1.461	1.470	.643	1.471	.693
4.091	1.469	1.476	.505	1.477	.541
4.454	1.473	1.480	.482	1.480	.498
4.634	1.474	1.480	.418	1.480	.421
5.933	1.455	1.445	-.704	1.443	-.810
6.386	1.438	1.418	-1.410	1.416	-1.563

[d,e] See footnotes on page 35.

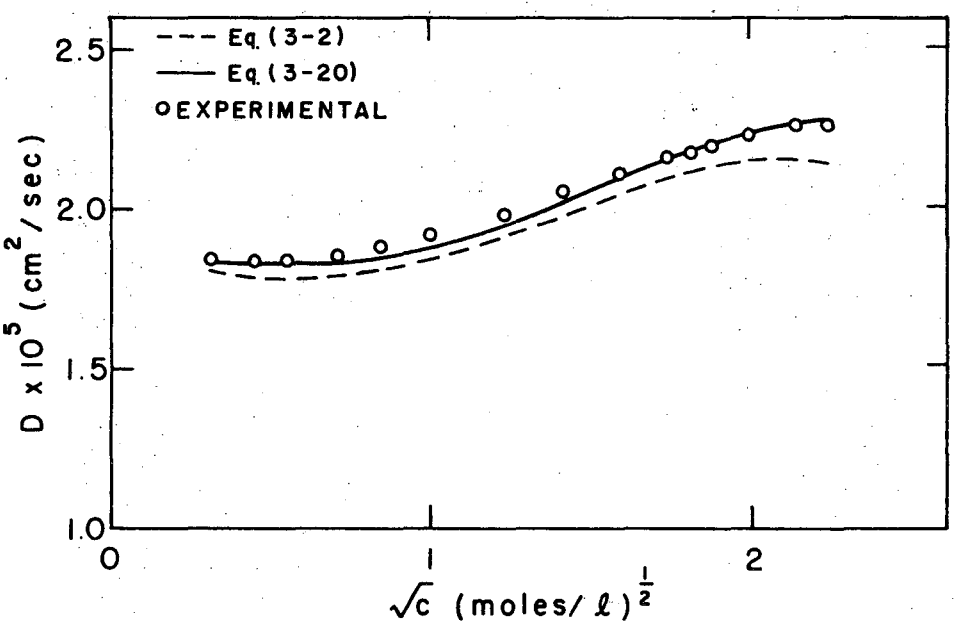

Fig. 3-12 Calculated and experimental diffusion coefficients of ammonium chloride in water at 25°C.

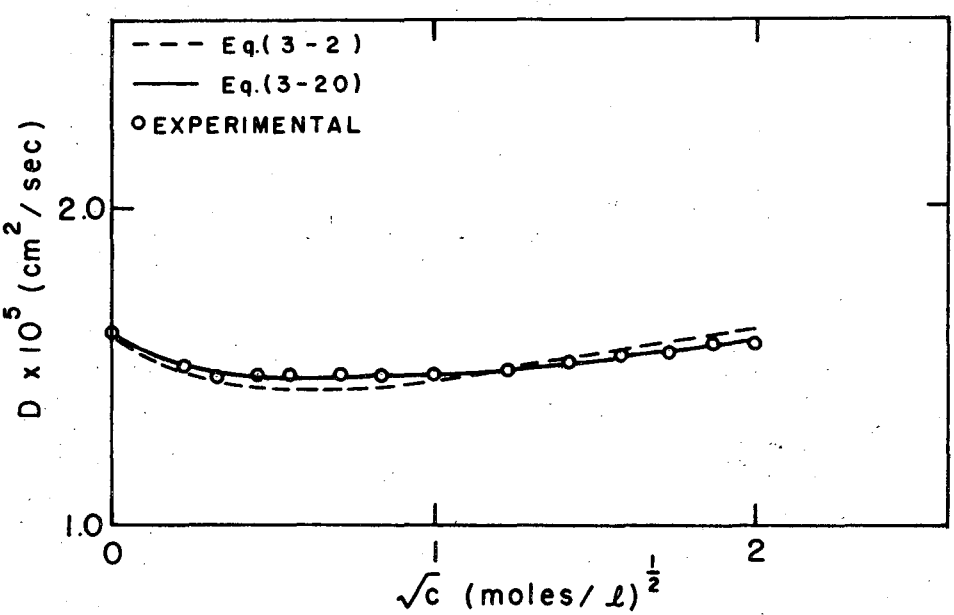

XBL 6911-6587

Fig. 3-13 Calculated and experimental diffusion coefficients of sodium chloride in water at 25°C.

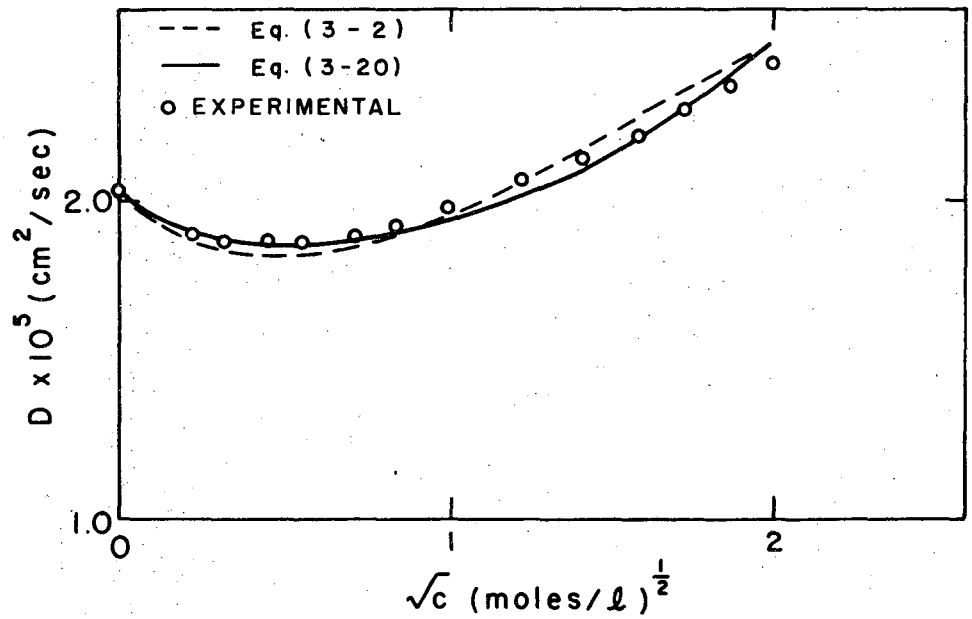

Fig. 3-14 Calculated and experimental diffusion coefficients of potassium bromide in water at 25°C.

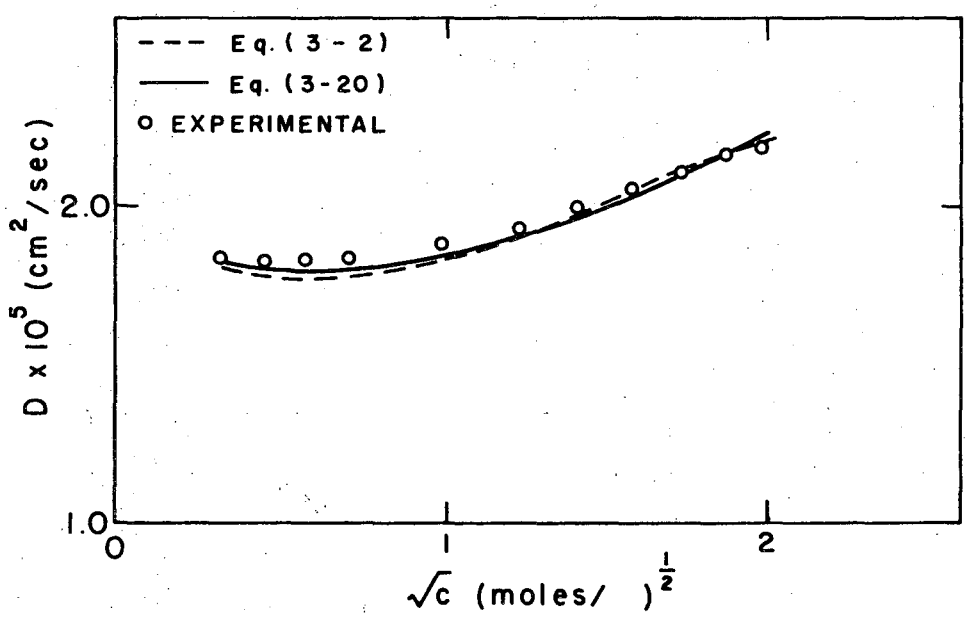

XBL 6911-6588

Fig. 3-15. Calculated and experimental diffusion coefficients of potassium chloride in water at 25°C.

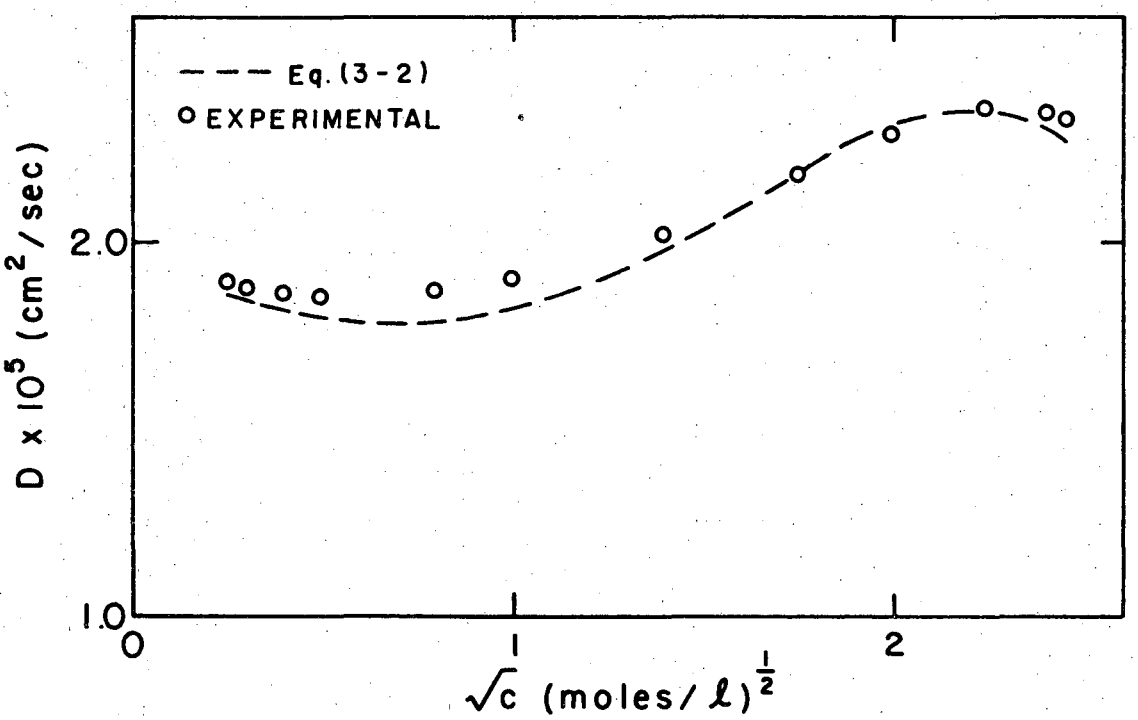

XBL 6911-6577

Fig. 3-16 Calculated and experimental diffusion coefficients of cesium chloride in water at 25°C.

obtains a straight line. Hence, the method can be used to estimate diffusivities if experimental data are available only for two concentrations simply by interpolating or extrapolating along the fit line. It also seems to be a convenient method to perform consistency tests on the reported diffusivity data.

C. Extention of the Rate Equation

In Section A we have seen that the $\eta\mathfrak{D}$ values stay constant for some electrolytic solutions, mostly of the alkali halide type, but for some other electrolytes they show negative or positive deviations especially at moderate and high concentrations. Unfortunately, most of the electrolytes are of the latter type. However, if we go back to Tables 3-6 through 3-9 and the corresponding figures for LiCl, KI, $CaCl_2$ and HCl, we observe that $\eta\mathfrak{D}$ remains fairly constant in dilute solutions, where these electrolytes are still close to ideal behavior. Deviations from the limiting value $\eta^{o}D^{o}$ are not that significant for LiCl, KI and $CaCl_2$ up to concentrations as high as 0.5 molar. The deviation starts at smaller concentrations for hydrochloric acid due to the strong structure making effect of the hydrogen ion. Other strong acids would be expected to show a similar behavior.

We make use of this observation by estimating diffusivities at low concentrations from Eq. (3-2) and extrapolate this information to higher concentrations by the method of Section B. In other words, we simply fit the logarithm of the equation,

$$\eta^{o}/\eta = e^{qp} \qquad (3\text{-}23)$$

to a straight line using viscosity data at low concentrations. We then substitute the computed slope q into either Eq. (3-20) or Eq. (3-22)

in an attempt to calculate diffusion coefficients at higher concentrations. Equation (3-23) actually follows from an incorporation of the results of Section A and B, or in mathematical terms, from the combination of Eqs. (3-1) and (3-15). In solutions where $\eta\mathcal{D}$ exhibits negative deviations, the $\eta\mathcal{D}_x$ values would prescribe a path closer to $\eta^o D^o$ than the $\eta\mathcal{D}_p$ values because of the reasons mentioned in Section A. Application of Eq. (3-22) would therefore be expected to yield more accurate results in such cases. Conversely, for cases where deviations are positive it would be more appropriate to employ Eq. (3-20). This argument adds a significant amount of empiricism to our already semi-empirical discussion, but we are somewhat justified in it when we consider the abundance of information as regards to the effects of different ions on the structure of water. We can use that information, such as the results of Chapman,[7] in order to predict the expected behavior of $\eta\mathcal{D}$ values.

We have fitted ln (η^o/η) versus the particle fraction by the method of least squares for LiCl, KI, $CaCl_2$ and HCl in Figs. 3-17 and 3-18. The fit was for concentrations between 0 and 0.5 molar for KI, $CaCl_2$, and LiCl, and between 0 and 0.1 molar for HCl. The circled points are not actually the measured experimental data, but were interpolated from available data using the correlation function for viscosity given in the Appendix. A major defect of such a fit is that experimental viscosity data are very scarce at the concentration range of interest. A few experimental points were available for KI, $CaCl_2$ and HCl at concentrations below 0.5 molar. Available viscosity data on LiCl, however, did not go below 1 molar; the values used for curve fitting were therefore interpolated from data at infinite dilution and high concentrations. Using such interpolated viscosity data is believed to introduce signi-

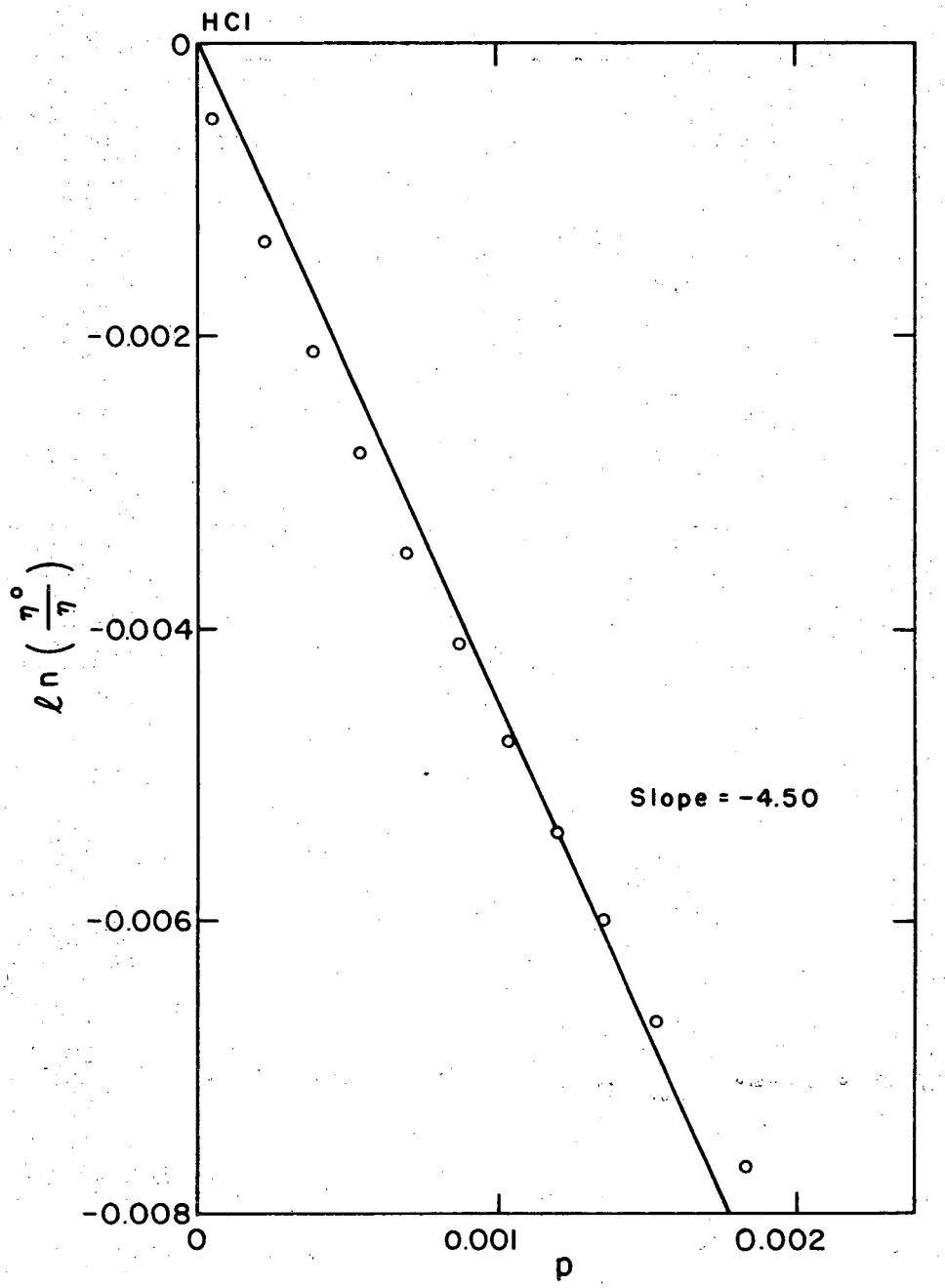

XBL 6911-6581

Fig. 3-17 Viscosity correlation for hydrochloric acid in water at 25°C.

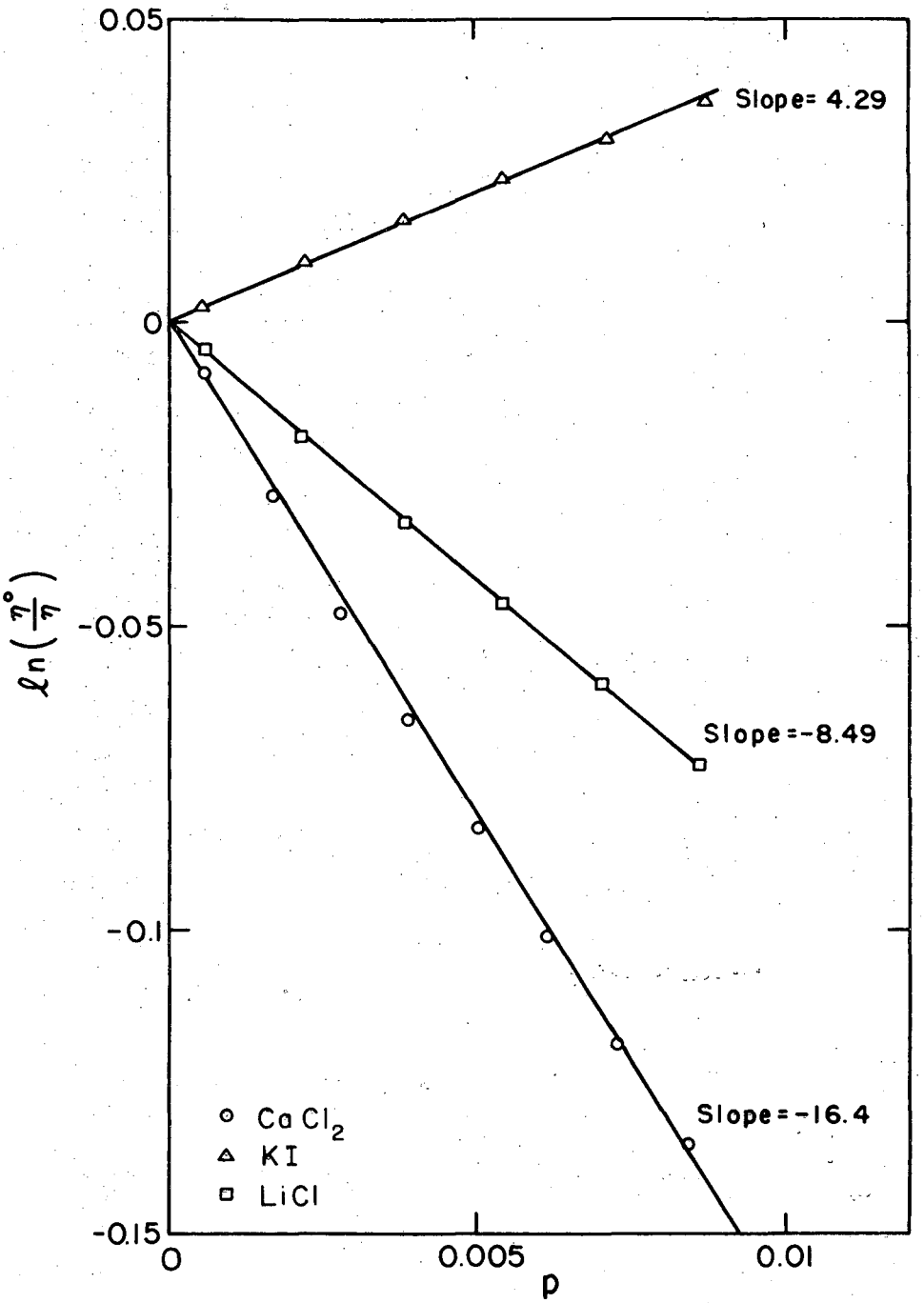

XBL 6911-6578

Fig. 3-18 Viscosity correlation for selected electrolytic solutions at 25°C.

ficant errors in the calculated diffusivities.

We substituted the slopes of fit lines into Eqs. (3-20) and (3-22) to compute the diffusion coefficients. Results from both equations are given in Tables 3-19 to 3-22. As was expected, Eq. (3-22) gives better results for $CaCl_2$, LiCl and HCl, whose $\eta\mathcal{D}$ curves exhibit negative deviations. On the contrary the results obtained from Eq. (3-20) are more satisfactory for KI, whose $\eta\mathcal{D}$ values show positive deivations. Calculated diffusivities of the four electrolyte systems are depicted in Figs. 3-19 through 3-22 and compared to the results of the previous sections. The curves indicate that the results obtained here provide a considerable improvement over the prediction of Eq. (3-2) for $CaCl_2$, HCl and KI. We could not accomplish a significant improvement over the results of Section A for LiCl. This is probably due to the inadequacy of the available viscosity data on lithium chloride at low concentrations.

Even though the rate equation model provides reasonable agreement with the experimental data, its general validity for electrolytic solutions may still be questionable because several important assumptions are concealed in the whole development. The treatment of Glasstone, et al. is probably over-simplified in liquids considering the complex behavior of electrolytic solutions. Their treatment and the extention of it to electrolytic solutions with the lattice model carry a number of assumptions that imply regular solution behavior. Furthermore, the physical significance of some of its parameters such as the specific rate constant and the activation free energy term remain in doubt and require extensive treatment by more sophisticated models on the structure of electrolytic solutions.

TABLE 3-19 Experimental and predicted diffusion coefficients of calcium chloride in water at 25°C.

EXP DATA ARE FROM LYONS & RILEY, JACS 76, 5216 (1954)

c	D_{exp}	D_{cal} [f]	% Error	D_{cal} [g]	% Error
.028	1.153	1.132	-1.843	1.131	-1.943
.055	1.136	1.096	-3.488	1.094	-3.679
.102	1.122	1.073	-4.406	1.069	-4.761
.193	1.123	1.069	-4.817	1.061	-5.489
.314	1.132	1.091	-3.645	1.078	-4.762
.469	1.152	1.133	-1.623	1.113	-3.346
.671	1.177	1.197	1.688	1.166	-.892
1.000	1.220	1.305	6.971	1.254	2.824
1.442	1.271	1.441	13.377	1.358	6.818
1.462	1.271	1.447	13.822	1.362	7.135
2.046	1.310	1.583	20.817	1.446	10.392
2.570	1.311	1.640	25.108	1.454	10.898
3.250	1.248	1.595	27.801	1.350	8.188
4.001	1.078	1.378	27.843	1.096	1.629
4.486	.919	1.163	26.595	.880	-4.272
5.012	.716	.898	25.357	.636	-11.276
5.424	.571	.691	20.975	.459	-19.670
6.004	.402	.440	9.415	.260	-35.342

[f] Calculated from Eqs. (3-23) and (3-20)

[g] Calculated from Eqs. (3-23) and (3-22)

TABLE 3-20 Experimental and predicted diffusion coefficients of hydrochloric acid in water at 25°C.

EXP DATA ARE FROM STOKES, JACS 72, 2243 (1950)

[illegible]	3.339	3.336	[illegible]	3.336	[illegible]
[illegible]	3.[illegible]	3.789	.5[illegible]	3.[illegible]	.839
[illegible]	3.[illegible]	3.871	.5[illegible]	3.[illegible]	.817
[illegible]	[illegible]	[illegible]	1.117	3.[illegible]	[illegible]
[illegible]	[illegible]	3.173	1.927	3.136	1.373
[illegible]	3.194	3.29[illegible]	3.321	3.26[illegible]	2.39[illegible]
[illegible]	3.29[illegible]	[illegible]	[illegible]	3.4[illegible]	3.4[illegible]
1.[illegible]	3.436	3.[illegible]	7.2[illegible]	3.52[illegible]	[illegible].364
[illegible]	3.7[illegible]	5.358	5.763	4.[illegible]	[illegible].862
2.[illegible]	[illegible]	[illegible]	12.373	4.396	9.3[illegible]
[illegible]	4.337	4.982	14.8[illegible]	4.7[illegible]	[illegible].9[illegible]
[illegible]	[illegible]	[illegible].421	14.3[illegible]	5.141	[illegible].371
3.[illegible]	[illegible]	[illegible]	[illegible]	[illegible]	11.[illegible]
[illegible]	[illegible]	[illegible]	[illegible]	[illegible]	13.247

[f,g]See footnotes on page 51.

TABLE 3-21 Experimental and predicted diffusion coefficients of potassium iodide in water at 25°C.

EXP DATA ARE FROM DUNLOF $ STOKES, JACS 73, 5456 (1951)

c	D_{exp}	D_{cal} [f]	% Error	D_{cal} [g]	% Error
-0.	2.001	1.999	-.100	1.999	-.100
.050	1.891	1.887	-.192	1.886	-.283
.100	1.865	1.880	.784	1.876	.602
.200	1.859	1.888	1.577	1.881	1.209
.300	1.884	1.906	1.171	1.896	.621
.500	1.955	1.949	-.330	1.931	-1.235
.700	2.001	1.994	-.374	1.968	-1.643
1.000	2.065	2.062	-.165	2.024	-1.988
1.500	2.166	2.172	.295	2.113	-2.470
2.000	2.254	2.272	.820	2.188	-2.910
2.500	2.347	2.350	.110	2.240	-4.551
3.000	2.440	2.388	-2.132	2.254	-7.638
3.500	2.533	2.371	-6.397	2.214	-12.582

[f,g] See footnotes on page 51.

TABLE 3-22 Experimental and calculated diffusion coefficients of lithium chloride in water at 25°C

EXP DATA ARE FROM VITAGLIANO, GAZ CHIM ITAL 90, 876(1960)

c	D_{exp}	D_{cal}[f]	% Error	D_{cal}[g]	% Error
.117	1.267	1.269	.185	1.267	-.027
.128	1.262	1.269	.555	1.266	.323
.168	1.261	1.269	.667	1.266	.364
.272	1.262	1.278	1.245	1.271	.750
.316	1.264	1.283	1.506	1.276	.930
.335	1.264	1.285	1.698	1.278	1.087
.422	1.269	1.298	2.299	1.288	1.525
.587	1.278	1.326	3.741	1.312	2.653
.660	1.280	1.339	4.617	1.323	3.385
.944	1.300	1.394	7.250	1.371	5.451
1.164	1.317	1.439	9.289	1.410	7.036
1.666	1.346	1.546	14.868	1.501	11.508
1.898	1.346	1.596	18.609	1.543	14.670
2.049	1.370	1.629	18.933	1.571	14.678
2.833	1.417	1.798	26.884	1.710	20.682
3.206	1.436	1.875	30.585	1.772	23.401
3.811	1.461	1.993	36.434	1.864	27.589
4.091	1.469	2.044	39.147	1.902	29.502
4.454	1.473	2.105	42.932	1.947	32.201
4.634	1.474	2.134	44.760	1.967	33.480
5.933	1.455	2.289	57.314	2.065	41.891
6.386	1.438	2.320	61.306	2.076	44.386

[f,g]See footnotes on page 51.

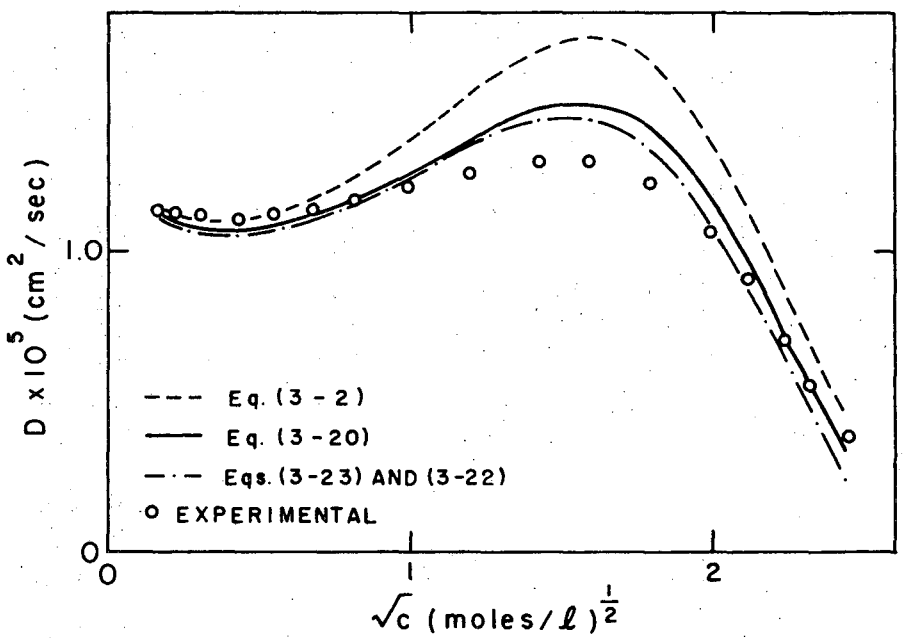

Fig. 3-19 Calculated and experimental diffusion coefficients of calcium chloride in water at 25°C.

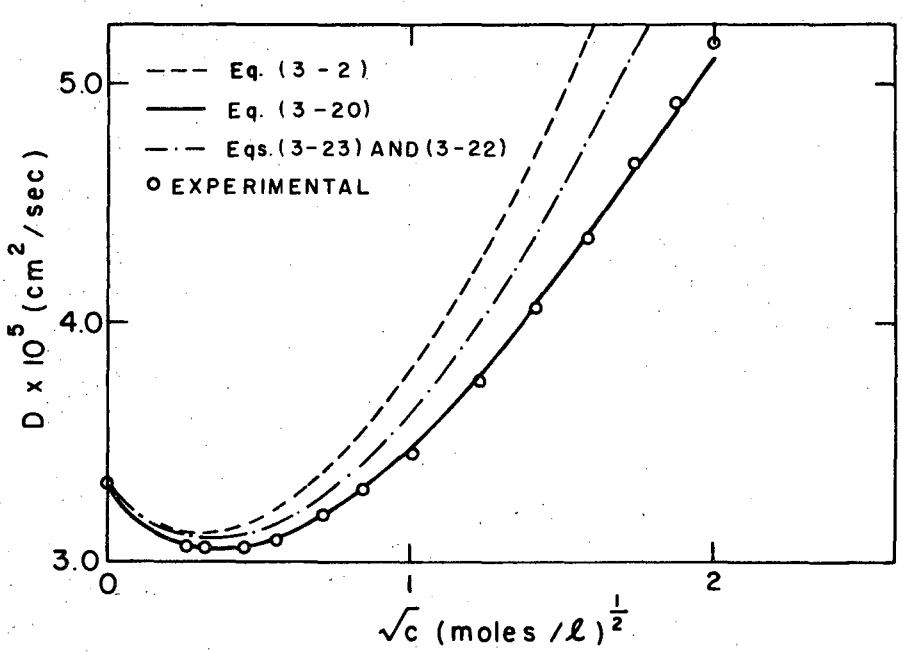

XBL 6911-6586

Fig. 3-20 Calculated and experimental diffusion coefficients of hydrochloric acid in water at 25°C.

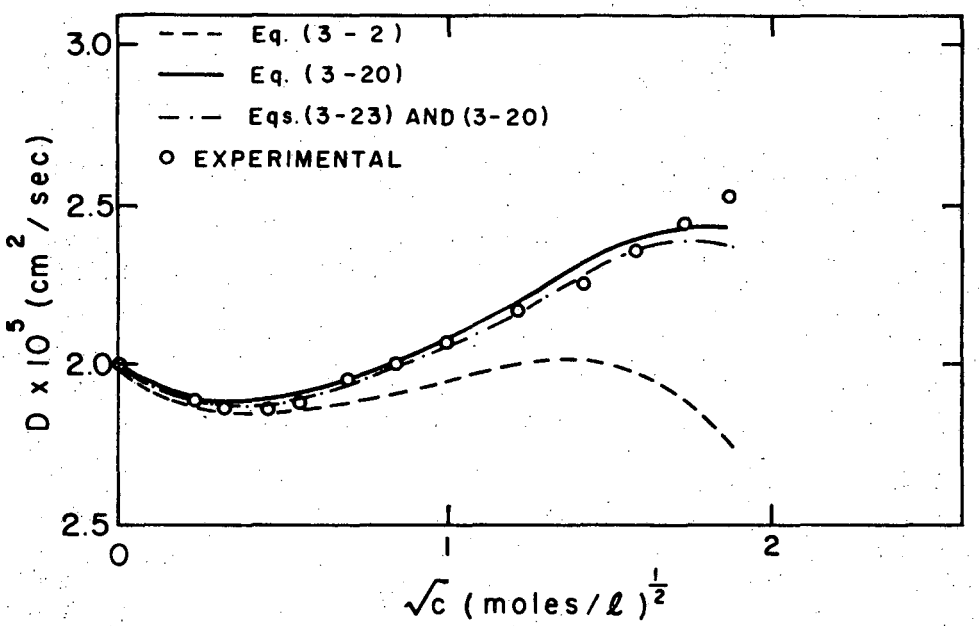

Fig. 3-21 Calculated and experimental diffusion coefficients of potassium iodide in water at 25°C.

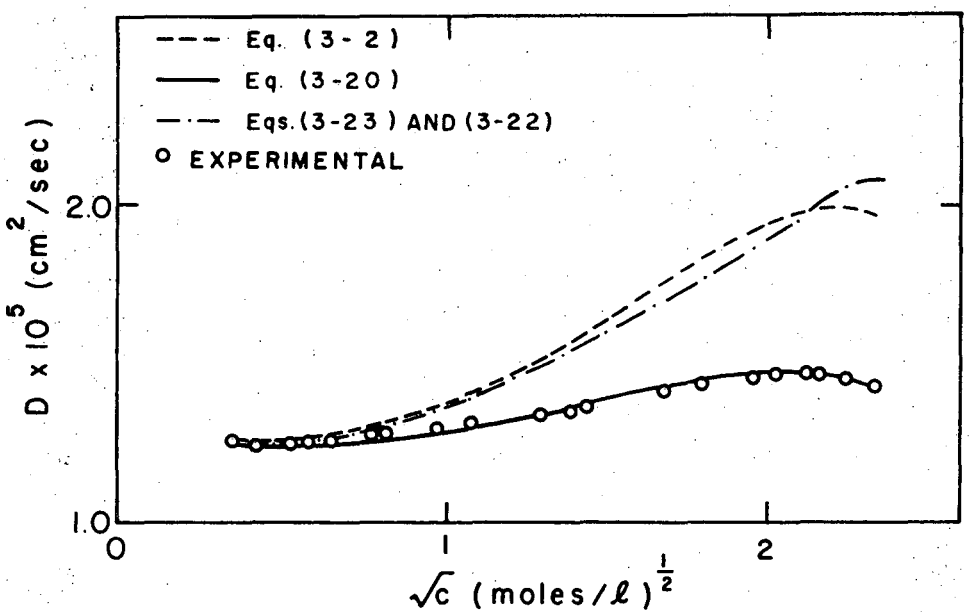

XBL 6911-6590

Fig. 3-22 Calculated and experimental diffusion coefficients of lithium chloride in water at 25°C.

We are curtailed from testing the methods discussed in this chapter for a wider selection of electrolytic systems, so that we could say more about their general applicability, due to limited experimental data on these systems.

In order to develop more reliable schemes for estimating the diffusion coefficients, it is necessary to have more data on the viscosities and diffusion coefficients. In the following chapters we discuss a method for measuring diffusion coefficients, which follows from the results of the theoretical developments of Chapter II. We use this method to measure the diffusion coefficients of nitric acid over a wide range of concentrations, thus completing the work started on this electrolyte by Chapman.[5] We also measure the viscosity of nitric acid in dilute solutions in order to complement already available data.

IV. A METHOD FOR THE MEASUREMENT OF DIFFUSIVITY - RESTRICTED DIFFUSION

A method of measuring differential diffusion coefficients in dilute electrolytic solutions via restricted diffusion has been first developed by Harned.[19] He proposed an approximate solution to Fick's second law applied to an enclosed column of liquid of fixed height. His solution assumes constant fluid properties in dilute solution and neglects the contribution of the solvent flux to the diffusion process. The first assumption could be a major source of error in Harned's experimental data because the fluid properties are known to undergo significant variations with concentration in dilute solutions. The second assumption would be a factor to be considered in concentrated solutions.

In order to determine the decay of concentration gradient with respect to time, Harned employed a conductimetric method. This method would impose additional drawbacks on the measurement of diffusivity in concentrated solutions. Solutions of high conductivities would require wider cells, inevitably increasing the effects of convection. Conductivities of some electrolytic solutions also fail to behave as linear functions at high concentrations. Harned's method, nevertheless, appears to be quite exact at low concentrations because the conductimetric method provides an accurate means of detecting small changes in concentration gradients in dilute solutions.

A vastly improved treatment of the restricted diffusion model has recently been developed by Chapman.[9] His solution of Fick's second law for the same model avoids Harned's assumptions. Chapman also proposed an optical method, utilizing Rayleigh interferometry, which overcomes

the restrictions of the conductimetric method at high concentrations and thus yields quite accurate diffusion coefficients in concentrated solutions. We will give here some of the details of Chapman's mathematical formulation of the problem and briefly discuss the fundamentals of Rayleigh interference.

A. Analysis of Restricted Diffusion

In Chapt. II we presented the expression for the fluxes of solvent and solute, viz. Eqs. (2-6) and (2-20), which are applicable for both dilute and concentrated solutions. In order to derive equations analogous to Fick's second law, we substitute these expressions into the conservation Eq. (2-1) and obtain

$$\frac{\partial c_o}{\partial t} = c_o \nabla \cdot \underline{v}_o - \underline{v}_o \cdot \nabla c_o \tag{4-1}$$

for the solvent, and

$$\frac{\partial c}{\partial t} = \nabla \cdot \left(\frac{D}{c_o \bar{V}_o}\right) \nabla c - c \nabla \cdot \underline{v}_o - \underline{v}_o \cdot \nabla c \tag{4-2}$$

for the solute. These may be rearranged as

$$\frac{\partial c}{\partial t} = \frac{\nabla \cdot \left(\frac{D}{c_o V_o}\right) \nabla c}{1 - \frac{c}{c_o} \frac{dc_o}{dc}} - \underline{v}_o \cdot \nabla c, \tag{4-3}$$

and

$$c_o \left(1 - \frac{c}{co} \frac{dc_o}{dc}\right) \nabla \cdot \underline{v}_o + \frac{dc_o}{dc} \nabla \cdot \left(\frac{D}{c_o \bar{V}_o}\right) \nabla c = 0. \tag{4-4}$$

It can be shown that[26]

$$\bar{V}_o = \frac{1}{c_o \left(1 - \frac{c}{c_o} \frac{dc_o}{dc}\right)}. \tag{4-5}$$

Equation (4-3) and (4-4) may be rewritten as

$$\frac{\partial c}{\partial t} = c_o \bar{V}_o \nabla \cdot \left(\frac{D}{c_o \bar{V}_o} \right) \nabla c - \underline{v}_o \cdot \nabla c, \tag{4-6}$$

and

$$\nabla \cdot \underline{v}_o + \bar{V}_o \frac{dc_o}{dc} \nabla \cdot \left(\frac{D}{c_o \bar{V}_o} \right) \nabla c = 0. \tag{4-7}$$

Equations (4-6) and (4-7) are now in a convenient form to solve for our one dimensional restricted diffusion model.

In setting up the boundary conditions for the problem, we realize that the fluxes should vanish at the bottom of the liquid column so that

$$v_o \Big|_{y=0} = 0 \tag{4-8}$$

and

$$\frac{\partial c}{\partial y} \Big|_{y=0} = 0 \tag{4-9}$$

where y is the displacement coordinate along the height of cell. At the top of the column the fluxes relative to the boundary vanish also, i.e.,

$$\frac{\partial c}{\partial y} \Big|_{y=a} = 0, \tag{4-10}$$

where a is the height of column. The law of conservation of mass for the system adds another boundary condition, namely,

$$\int_0^a \rho dy = \int_0^{a^\infty} \rho^\infty dy = a^\infty \rho^\infty \tag{4-11}$$

The superscript refers to conditions at infinite time, when the diffusing system reaches a uniform concentration.

The problem can be solved by a series method. We assume that the unknown parameters can at large times be represented by singular perturbation expansion series of the form

$$c = c^\infty + \epsilon c^{(1)} + \epsilon^2 c^{(2)} + \ldots, \tag{4-12}$$

$$a = a^\infty + \epsilon a^{(1)} + \epsilon^2 a^{(2)} + \ldots, \tag{4-13}$$

and

$$v_o = \epsilon v_o^{(1)} + \epsilon^2 v_o^{(2)} + \ldots, \tag{4-14}$$

where the perturbation parameter ϵ is defined as a function of time and obeys the condition that

$$\epsilon \Big|_{t=\infty} = 0. \tag{4-15}$$

The coefficients $c^{(i)}$, $a^{(i)}$ and $v_o^{(i)}$ are independent of time. Therefore $c^{(i)}$ and $v_o^{(i)}$ depend only on position. In order to account for the concentration dependence of the diffusion coefficient we expand this quantity in terms of Taylor series around c^{∞} and write

$$D = D^{\infty} + \frac{dD}{dc}\Big|_{c^{\infty}} (c-c^{\infty}) + \frac{1}{2} \frac{d^2D}{dc^2}\Big|_{c^{\infty}} (c-c^{\infty})^2 + \ldots, \tag{4-16}$$

where $D^{\infty} = D(c^{\infty})$.

Substitution of Eqs. (4-12) through (4-14) into Eqs. (4-6) through (4-11) and equating terms of equal order in ϵ accomplishes a separation of variables by yielding a number of differential equations with corresponding set of boundary conditions. These equations can be solved simultaneously to determine ϵ and the coefficients $c^{(i)}$, $a^{(i)}$ and $v_o^{(i)}$. The ability to generate such equations justifies the assumptions involved in Eqs. (4-12) through (4-16).

Equating the terms of first order in ϵ in the expansion of Eq. (4-6) gives, for example,

$$\frac{d\epsilon}{dt} c^{(1)} = D^{\infty} \epsilon \frac{d^2c^{(1)}}{dy^2} \tag{4-17}$$

with the boundary conditions,

$$\frac{dc^{(1)}}{dy}\Big|_{y=0} = 0, \tag{4-18}$$

and

$$\frac{dc^{(1)}}{dy}\Big|_{y=a^{\infty}} = 0. \tag{4-19}$$

Solving Eq. (4-17), we obtain

$$\epsilon = e^{-D^{\infty}t\,(\pi/a^{\infty})^2} \tag{4-20}$$

and

$$c^{(1)} = A \cos\,(\pi y/a^{\infty}), \tag{4-21}$$

which satisfy the two boundary conditions and the condition expressed by Eq. (4-15). A is a constant to be determined from the initial conditions which have been left as arbitrary. The parameter a has been replaced by a^{∞} because order of magnitude estimations show that the variation in a is negligible.[10] The complete solution is very complicated, and we will avoid here the rest of the algebraic manipulation. The reader is referred to the original work by Chapman[10] for a more detailed analysis.

An important result is

$$\Delta c = c(a/6) - c\,(5a/6)$$

$$= A\sqrt{3}\;e^{-D^{\infty}t(\pi/a)^2} + B\,e^{-3D^{\infty}t(\pi/a)^2} + \ldots, \tag{4-22}$$

where we have taken the difference in concentration between points one-sixth of the overall length from each end of the cell so that the trigonometric terms in the series are reduced to constants. The coefficient B depends in a complicated way on the initial condition and the derivatives of solution properties. At large enough times the higher order exponential terms become negligibly small as compared to the first term, thus reducing the solution to the simple results expressed by Eqs. (4-20) and (4-21). At large times, we can therefore write

$$\Delta c = A'\,e^{-D^{\infty}t\,(\pi/a)^2} \tag{4-23}$$

where $A' = A\sqrt{3}$. Equation (4-23) is now in convenient form to determine differential diffusion coefficients from experimental data on Δc versus t.

B. Analysis of Rayleigh Interference

Consider a coherent beam of light passing through a pair of slits A and B (see Fig. 4-1) and projecting on a screen S at a distance R away from the slits. The rays emanating from the slits are initially in phase with each other, but phase changes due to diffraction occur at far enough distances from the slits depending on the distance each beam has traversed. The beams are in phase when the difference in their path length is an integral multiple of the wavelength λ, so that

$$d \sin \theta_m = m\lambda, \tag{4-24}$$

where d is the spacing between the slits and $\theta_m = \tan^{-1} (y/R)$. This condition corresponds to an intensity maximum on the screen. The condition,

$$d \sin \theta_m = (m + 1/2)\lambda, \tag{4-25}$$

causes an intensity minimum since the rays are 180° out of phase as they reach the screen. The sharp deviations in intensity thus create a pattern of light and dark fringes on the screen.

If we now place two different media of the same thickness ℓ behind each slit, we introduce an intial phase difference between the two rays as they pass through the mask. As a result the fringes are shifted depending on the initial deviation in the path lengths of the beams, and this deviation is in turn proportional to the difference in the refractive indices $\mu_A - \mu_B$ of the two media. The intensity maxima will then appear on the screen according to the condition that

$$d \sin \theta_m + \ell (\mu_A - \mu_B) = m\lambda. \tag{4-26}$$

If we fix μ_B and vary μ_A, we obtain at the point M on the screen,

$$\ell \Delta \mu_A = \lambda \Delta m, \tag{4-27}$$

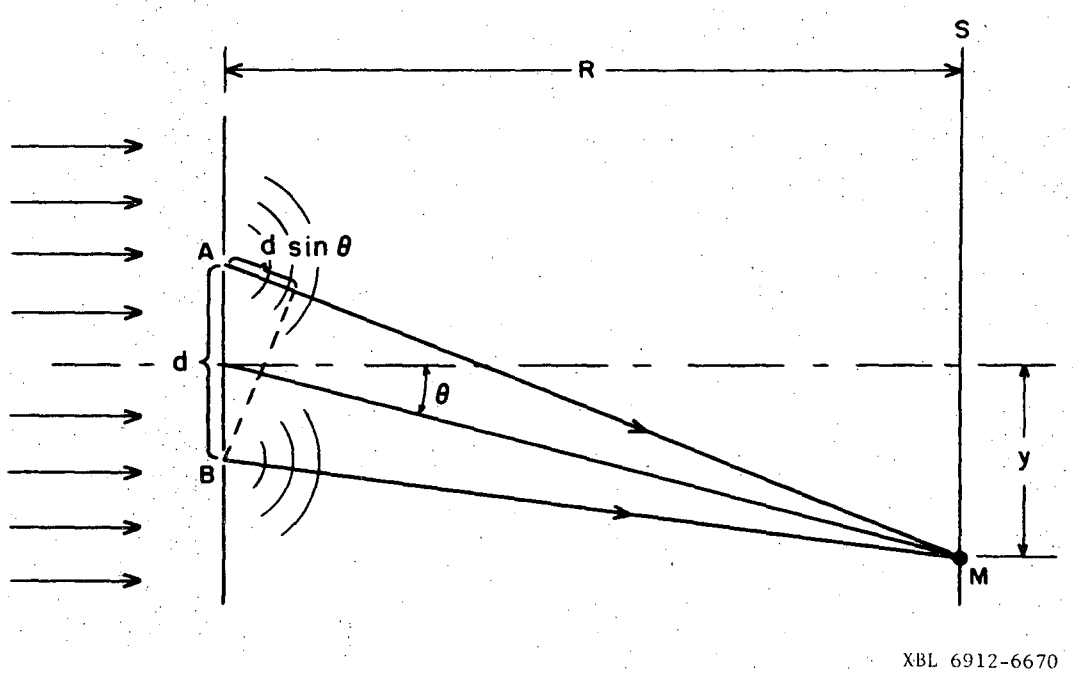

Fig. 4-1 Interference of monochromatic light by two slits.

indicating that a change in the refractive index of a diffusing system can be determined by observing the change in the order of fringe shifts. If $\Delta \mu_A$ is a linear function of concentration, the concentration changes in our system can be identified by the number of fringe shifts Δm. Chapman[11] estimates that the accuracy is better than 10^{-3} moles/l for potassium chloride solutions employing the experimental apparatus and technique to be discussed is the next chapter. As long as $\Delta\mu$ remains directly proportional to Δc, the method should work quite as accurately for most of the other electrolytic solutions.

V. EXPERIMENTAL WORK

In this chapter we describe the apparatus and the experimental method employed to measure the diffusion coefficients and the viscosities of aqueous nitric acid solutions at 25°C. We refer quite frequently to theses by Chapman[12] and Hsueh[22] who have used the same optical system as ours and performed quite similar experiments. We note the important differences between their work and ours. We direct the reader to these references for additional discussion, illustrations and bibliography.

A. Description of the Apparatus

1. Optical System

Diffusion experiments were performed on a Perkin-Elmer Model 238 Electrophoresis Apparatus. This is a compact instrument embodying a constant temperature bath, an optical chamber and a camera.

The bath is conveniently constructed so that the diffusion cell can be mounted in alignment with the optical path. It is equipped by a centrifugal pump to stir the bath fluid and a cooling plate connected to an air cooled refrigeration system. To these we added a 125-watt heating probe and an Inspector 445 thermometric element, both attached to a Sargent, Model S proportional temperature controller. The bath temperature was read on a Beckman thermometer. The controller system regulated the bath at 25.00±0.01°C.

The optics of the apparatus is somewhat complicated. Chapman gives the details in this respect. The optical set up is depicted in a simplified form in Fig. 5-1. The mercury vapor lamp emits a monochromatic light beam of wavelength 5461Å. A multipoint source slit is positioned in front of the lamp in order to intensify and space the interference patterns equally. The converging lens projects the beam through the solution and

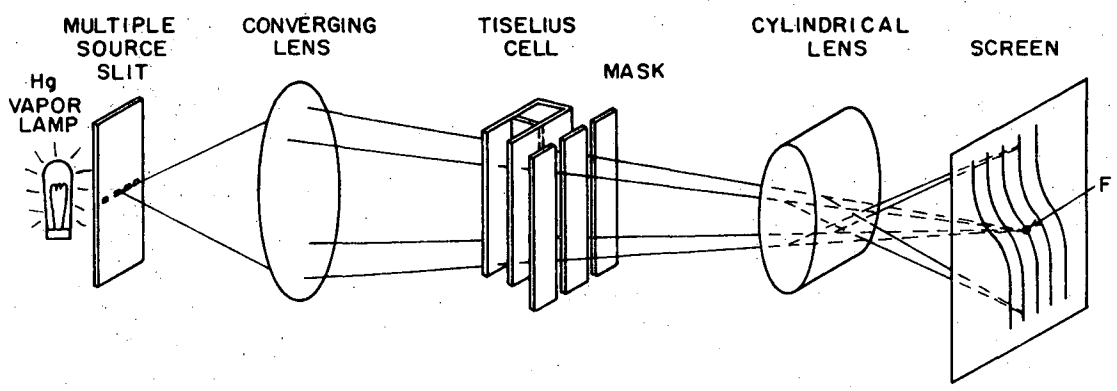

XBL 6912-6672

Fig. 5-1 A simplified Rayleigh interferometer.

reference components of the cell. The interference patterns formed by two slits placed behind the cell are focused on the screen and spread along a horizontal line containing the point F. As a result the contributions from different locations in the cell are superimposed so as to obscure the variations in the refractive index of the solution along a vertical path. The situation is improved by placing a cylindrical lens between the slits and the screen. The cylindrical lens spreads the fringes vertically. It thus adds a second dimension to the interference patterns by mapping them on the screen as profiles of refractive index with respect to position.

The fringe patterns produced by the optical system were photographed by a Polaroid Land Camera attached at one end of the apparatus. The photographs were taken on Polaroid Type 46L transparencies. Exposure times of about thirty seconds were used.

2. Optical Cells

The optical cells used in this work are of the Tiseluis type and were purchased from the Perkin-Elmer Corporation. A complete cell contains several parts, and these are explained in detail by Chapman. In our experiments we only used the center section which is shown in Fig. 5-2. It consists of two rectangular channels, mounted between flat, ground glass flanges. The faces of the cell are extended to the sides to be included in the optical reference path. The spaces between these extended portions are occupied by the bath fluid (distilled water in this case) and thus form the reference as shown in Fig. 5-1. Each channel can then be used as a different diffusion cell with its own reference compartment.

The height of the cells was of the order of 7.9 cm. Since Eq. (4-23) depends on this dimension quite significantly, it had to be measured as

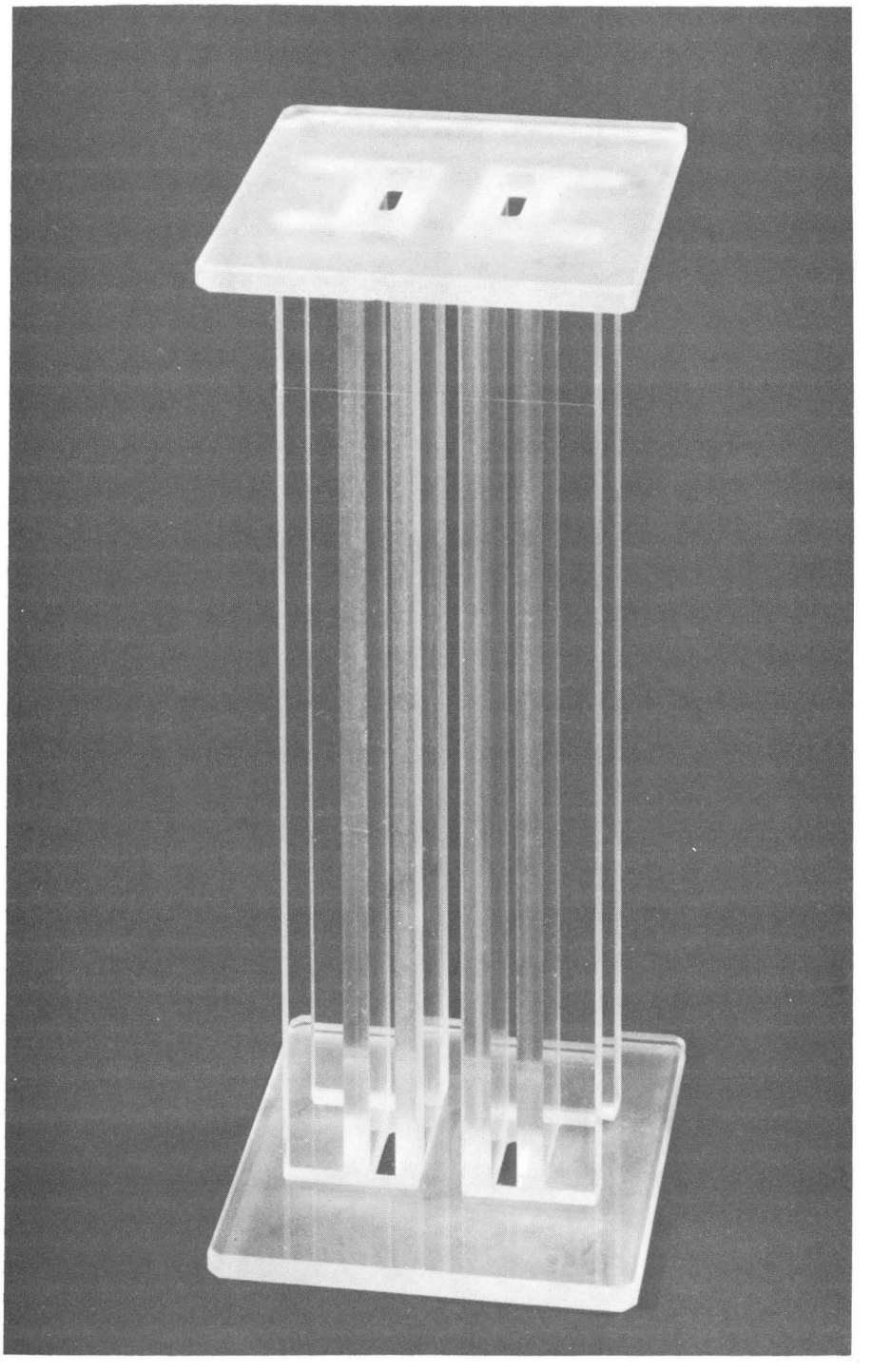

XBB 678-4586

Fig. 5-2 Central optical cell

accurately as possible. The Precision Shop of the Lawrence Radiation Laboratory measured the cell lengths within 0.03 percent. The width and the depth of a channel were 2 mm and 9 mm along the optical path respectively. These dimensions are an improvement over the Harned cell in reducing the effects of convection. The same shop also inscribed very fine markings on one face of the cell at exactly one-sixth of the overall length from each end of the cell. These resolved as fine lines across the photograph of the fringes and served as reference points for the measurement of concentration changes.

We used two glass pieces, ground on one side, in order to seal the cell at both ends before a diffusion run. These pieces were cut into the same size and thickness as the cell flanges.

The cell was placed into the bath in an appropriately designed cell holder. The cell rests on the bottom of the holder while spring tension is applied on the top. It is thus clamped firmly in position to avoid any leakage to and from the bath during a diffusion experiment.

The assembly and uses of the complete cell can be found in References 12, 22 and 26.

3. Boundary Forming Apparatus

The filling of the Tiselius cell before starting a diffusion run requires special care since it is desirable to form a fairly sharp boundary between the diffusing solutions at the outset. The boundary forming apparatus, which consists of a Motor-Driven Syringe Compensator Assembly and a Needle Controller Assembly, both supplied by Perkin-Elmer, is of great utility for this purpose. The former assembly contains a built-in constant speed motor which drives a 10 cc plunger. The travel rate of the plunger can be set at speeds as low as 0.015 cc per minute, or if necessary, the system

can be operated manually. This apparatus functions as a slow-speed pump in adding solution to the cell. The syringe is connected by a thin rubber tubing to a 2 ml pipette with 0.1 ml graduations. A hypodermic needle is attached to the narrow end of the pipette. The pipette is in turn clamped to the Needle Controller Assembly. The needle can be manually raised or lowered by means of a chain drive mechanism. Uses of the pipette are as a container and a volumetric measuring unit for the solutions to be added to or withdrawn from the cell. The whole system provides a convenient means of filling the cell by minimizing such disturbances on the boundary as inconsistant filling rates and sudden jerks of the needle.

The hypodermic needles (gage 18) were manufactured from a 90% platinum and 10% ruthenium alloy which is resistant to the corrosive effects of concentrated nitric acid solutions. The needles were purchased from the Hamilton Co. of Whittier, California.

4. Miscellaneous Apparatus

The fringe shifts were measured from Polaroid transparencies on a Jarrell-Ash Recording Microphotometer. Hsueh describes the optical set-up and the principles of operating this apparatus. Description of its use for this work will be given in the next section.

Viscosities of dilute nitric acid solutions were determined by Ostwald viscosimeters. These were calibrated with distilled water at 25°C.

B. Experimental Procedure

1. Diffusion Runs

In preparation for a run, the most important step was to clean the cell and the glass pieces carefully in order to remove undesirable impurities and spots that might interfere with the optical path. The grease from a

previous run was wiped out by a tissue paper wetted in cyclohexane. The cell was then washed in a solution of Alconox and rinsed with tap water. In order to remove rough dirt, the channels were washed with a pipe cleaner, one end of which was bent into a swirl so that the wire tip was not exposed. For further cleaning the cell and its glass covers were soaked in chromic acid cleaning solution for several minutes, then rinsed in distilled water and left to dry in an oven at 70°C.

For sealings chemically inert Apiezon Type N vacuum grease was employed. The grease was applied as a thin layer on the cell flanges, taking care so as to avoid getting any grease into the channels. A glass pieces was pressed against one of the flanges to seal the bottom of the cell.

The channels were then filled half way to the top by the heavier solutions. Care was taken not to trap any air bubbles at the bottom. Lighter solutions were added gently on top with the use of the boundary forming apparatus. The syringe plunger was coated with high vacuum silicon grease to avoid air leaks into the control volume generated by the syringe, rubber tubing and the 2 ml. pipette. The plunger speed was set depending on the initial concentration gradient at the boundary . In dilute solutions, for example, where the initial concentration difference had to be as low as 0.2 molar, the filling rate was set at 0.04 cc/minute. As the boundary was formed, and the liquid level rose in the channel, the needle tip was raised gradually away from the boundary at the same time increasing the plunger speed. At high concentrations where we could afford initial concentration differences as high as one molar, the plunger system could be driven manually at faster speeds. Higher filling rates did not disturb the boundary because the density gradients were large enough to stabilize the

liquid against convection currents. After both channels were filled completely, the cell top was sealed by sliding the second glass piece firmly over the top flange from one edge to the opposite, in the direction of the cell depth. This has to be done fast enough to avoid the intermixing of the channel contents at the top. The cell was then mounted in the cell holder and placed in the bath.

Simplicity of the procedures for cell filling are improvements over Chapman's experimental method. The boundaries formed by our method were considered to be sufficiently sharp so that it was deemed unnecessary to withdraw solution from the middle of a cell channel in order to form a sharper boundary.[13] A photograph of the fringe patterns soon after boundary formation is depicted in Fig. 5-3. This can be compared with a similar photograph in Chapman's thesis.[14]

Probably the most important improvement over Chapman's method is due to the simplication of the cell assembly, which allows the performance of two diffusion experiments at the same time. By avoiding the use of top and bottom sections of the cell, we also escaped some of the problems encountered by Chapman such as nonuniform tensions exerted by the holder on the cell. Such tension may cause leaks between the flanges and even lead to fractures within the cell body.

As mentioned earlier and also suggested by Chapman, we chose to form boundaries between solutions of appreciable concentration differences, such as one molar, so that a large density difference would act to reduce convection during boundary forming and cell mounting procedures. The decay of such a concentration difference required about two days before useful measurements could be taken; large concentration differences cause so many fringe shifts that the bending fringes are too close to be resolved

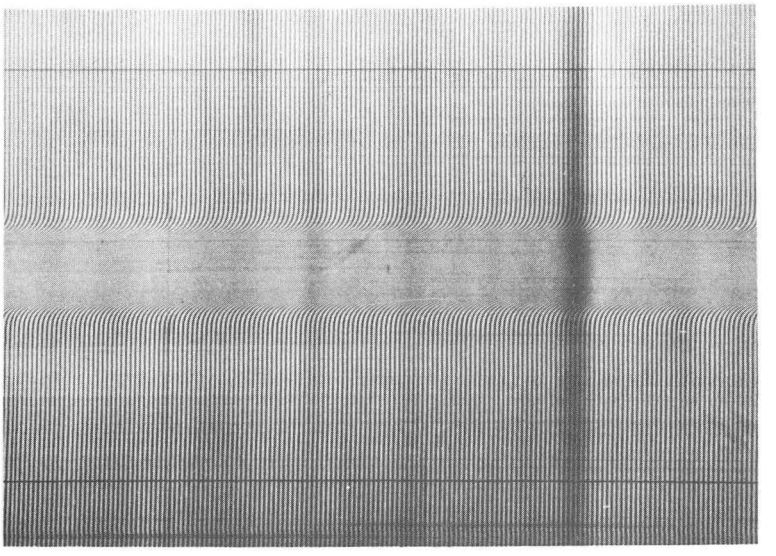

Fig. 5-3 Fringe patterns soon after boundary formation

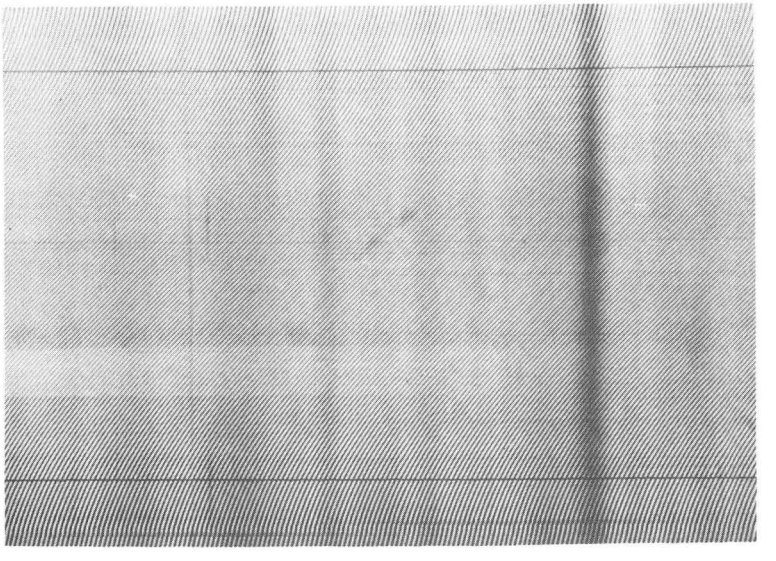

XBB 6911-7618

Fig. 5-4 Typical fringe pattern during data collection

(see Fig. 5-3). In dilute solutions, however, we were forced to work with smaller concentration differences during boundary formation, and this required greater care. Concentration differences less than 0.4 molar resolved workable fringe patterns soon after boundary formation, but the condition that Eq. (4-23) is applicable at large times, rendered this information useless. Even though the fringes may be resolvable at the very outset of a diffusion run, one has to allow for a minimum time lapse of about half a day before the higher order terms in Eq. (4-22) become negligible.

After the concentration gradient in a cell reached a convenient magnitude, and the conditions of Eq. (4-23) were met, photographs of the fringe patterns were taken at about two-hour intervals except over the night when the interval reached ten hours. Such measurements on a run were made over a period of 3000-4000 minutes. This time span was shorter for runs in dilute solutions because the concentration differences were quite low initially, and we had to terminate measurements sooner. We also had to take photographs in smaller intervals in order to secure sufficient data in a shorter period of time.

At the end of a run the cell was removed from the bath and shaken gently to attain a complete mixing of the contents of each channel. The solutions were withdrawn separately through hypodermic needles into clean 2 ml. pipettes attached to the boundary forming apparatus. About 1.1 cc of each solution was measured into a small flask and titrated to determine the value of c^{∞}.

The samples were prepared from Baker reagent grade nitric acid solution by diluting it with CO_2 free distilled water to the desired concentration. In preparing solutions below one molar, double distilled water was used

to attain a higher purity. Titrations were performed with standardized 0.1000 N sodium hydroxide solution to the phenolphthalein endpoint. The carbonate free hydroxide solution was prepared from a concentrate supplied by Anachemia Chemical Co.

2. Data Evaluation

A typical fringe pattern used to determine the concentration change with time is shown in Fig. 5-4. The horizontal lines across the patterns result from the reference marks on the cell. Each curve in the pattern represents the refractive index profile. It may also be regarded as a concentration profile if the refractive index varies linearly with concentration. The concentration difference between the two reference lines is proportional to the number of fringes, which are shifted across a vertical line between them, as implied by Eq. (4-27). Since the fringes are equally spaced, the concentration difference is also proportional to the horizontal displacement of a fringe between the two lines. Hsueh actually counts the number of fringe shifts across a vertical line to measure the concentration difference. This method poses some difficulties in the determination of fractional portions of fringes at the intersections with the reference lines. Chapman proposes a more accurate method, based on the measurement of the horizontal fringe displacement, which we adopt here.

The Polaroid transparency was placed on the traveling stage of microphotometer so that a light beam passing through it magnified and projected the fringes on a screen. The photograph was adjusted to set the reference lines parallel to the direction of longitudinal travel on the stage. The intersection of a dark fringe and a reference line was made to coincide with

a reference point marked on the screen. The position of the stage was read on the vernier scale. This scale measures the longitudinal displacement of the stage within 0.01 mm. The stage was then driven manually by turning the driving knobs as the projection of the chosen fringe was followed visually across the screen until it intersected the other reference line. The intersection line was brought to fall upon the same reference mark on the screen, and the longitudinal coordinate of the stage was recorded from the vernier. The difference of the two measurements yielded the horizontal displacement of a fringe between two reference lines to an accuracy of about 0.2 percent.

Equation (4-23) suggests that at large times the logarithm of the concentration difference between the reference lines should vary linearly with time and exhibit a slope of $-D(\pi/a)^2$. We have omitted the superscript on D for simplicity. The logarithm of the longitudinal fringe displacement Δ should also vary linearly with time exhibiting the same slope since Δ was measured as a quantity directly proportional to the concentration difference. We can therefore fit $\ln \Delta$ versus t with a straight line to determine the slope and then calculate the diffusion coefficient from the relation

$$D = -(\text{slope})\ (a/\pi)^2. \qquad (5\text{-}1)$$

C. Results and Discussion

1. Differential Diffusion Coefficients

We have measured the differential diffusion coefficients of nitric acid solutions for the concentration range 0 to 10 molar. In this range one can find sufficient and adequate data on density, viscosity, transference number, conductivity and activity coefficient in the literature.[15]

This information and our results on diffusion coefficients provide a complete set of data for study of transport in nitric acid solutions.

The refractive index of nitric acid in the concentration range of interest is nearly a linear function. It exhibits a maximum at around 14 molar[42] ; our experimental method would thus fail to work in that vicinity. Even so, this condition is an improvement over Harned's conductimetric method because the conductivity of nitric acid goes through a maximum at a lower concentration of about 6 molar.[15]

A typical semi-logarithmic plot of the fringe shift versus time is shown in Fig 5-5. The points fit smoothly to a straight line justifying the assumptions concealed in Eq.(4-23). In some of our runs we observed deviations from the least squares fit line. Negative deviations were sometimes detected at the small time end of the curve. These probably resulted from contributions of higher order terms in Eq. (4-22). Two types of deviations occasionally appeared at long times. The negative type was either caused by leaks at the bottom of the cell or by convective effects induced due to vibrations in the system when the density gradient became too small to prevent these effects. Leaks could usually be detected by observing unusal distortions in the fringe patterns. As long as there were no leaks, the fit curve could be corrected for these negative deviations at small and large times by simply discarding such points. The positive deviations, which we observed quite often at large times, could not be corrected for even if we tried discarding data points measured at large times and recalculating the diffusion coefficient. In all cases such deviations resulted in a too low value for the diffusivity so that we had to repeat the whole run. The factors causing this type of deviations are not obvious,

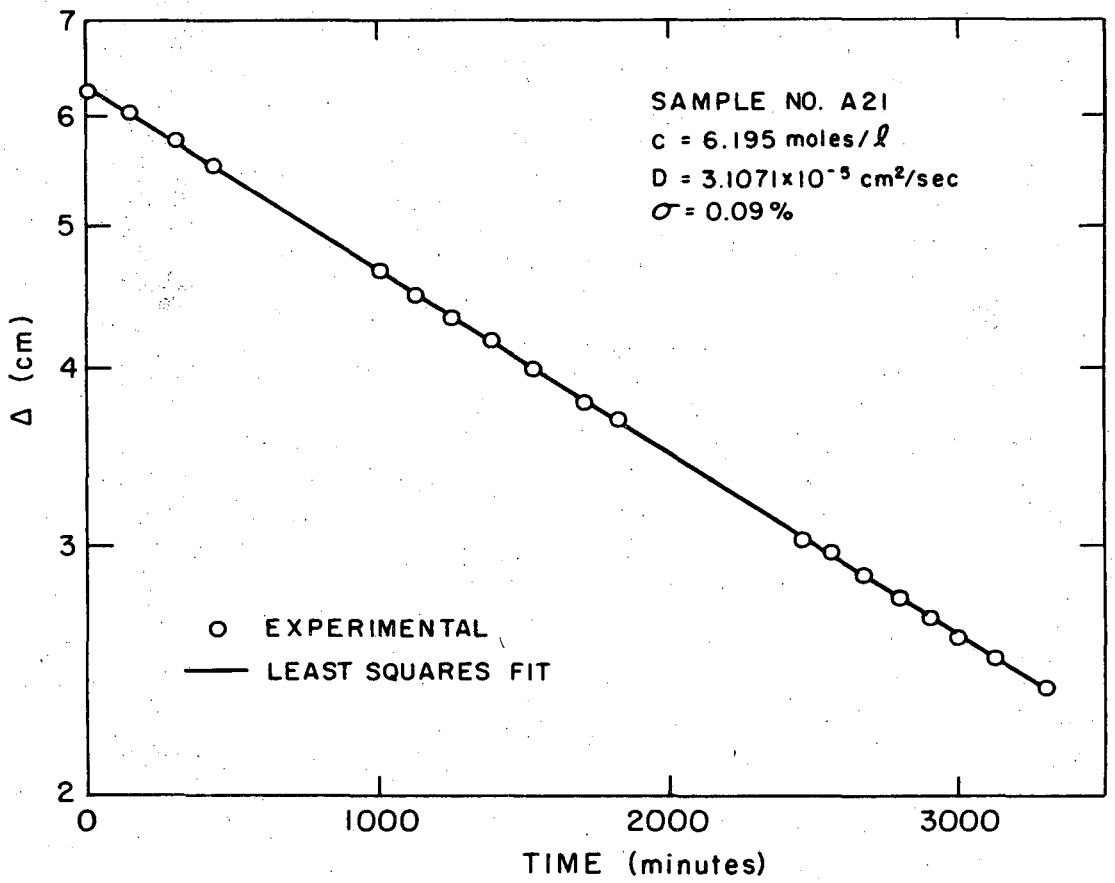

XBL 6912-6673

Fig. 5-5 Sample data analysis for diffusion of nitric acid in water at 25°C. σ is the estimated error in the diffusion coefficient.

but we can speculate on several possibilities. Presence of certain organic impurites could interfere with the refractive index of the solution even though the cell was cleaned and solutions prepared with maximum care to avoid undesirable contamination. The dissolution of grease in solution can be ruled out because we performed preliminary tests to confirm that nitric acid does not attack the Apiezon grease to any significant extent. However, we have observed some degree of absorption of acid by a thin layer of grease coated on a glass piece. This phenomenon appears to be a physical interaction because the absorbed amount can be extracted completely upon equilibration in vacuum. Absorption is probably enhanced by the presence of air cavities which may be trapped within the grease layer during sealing of the cell. If a significant amount of the solution thus leaks into the space formed by air cavities, it may provide the grounds for a positive deviation. Such a leak would not cause any visible distortions in the fringe pattern. Another possible cause may be an actual leak and mixing with the bath fluid at the top of the cell, but this kind of an effect could not be observed to occur from examinations of the interference patterns.

The results of diffusion runs are summarized in Table 5-1. These are compared with Chapman's results in Fig. 5-6. The agreement is within the precision of our method at one point only. The other points deviate from our interpolated values by as much as 1.5 percent.

The variance in the slope of fit line was calculated according to a standard statistical formula[25] to determine the degree of confidence in the calculated diffusion coefficient. In most runs the estimated error in the diffusion coefficient was below 0.1 percent. As can be seen from

TABLE 5-1 The diffusion coefficient of nitric acid in water at 25°C

c(moles/ℓ)	$D \times 10^5 (cm^2/sec)$	% Error[25]
0.033	2.835	0.38
0.110	2.782	0.19
0.199	2.774	0.13
0.256	2.786	0.05
0.265	2.780	0.11
0.414	2.805	0.07
0.499	2.815	0.05
0.515	2.806	0.07
0.629	2.837	0.06
1.006	2.939	0.08
1.020	2.939	0.04
1.505	3.045	0.05
1.797	3.119	0.11
2.030	3.148	0.06
2.090	3.158	0.18
2.375	3.203	0.17
2.586	3.224	0.06
3.039	3.268	0.10
4.187	3.317	0.08
5.253	3.233	0.08
6.195	3.107	0.09
7.450	2.921	0.07
8.40	2.778	0.07
9.25	2.642	0.08

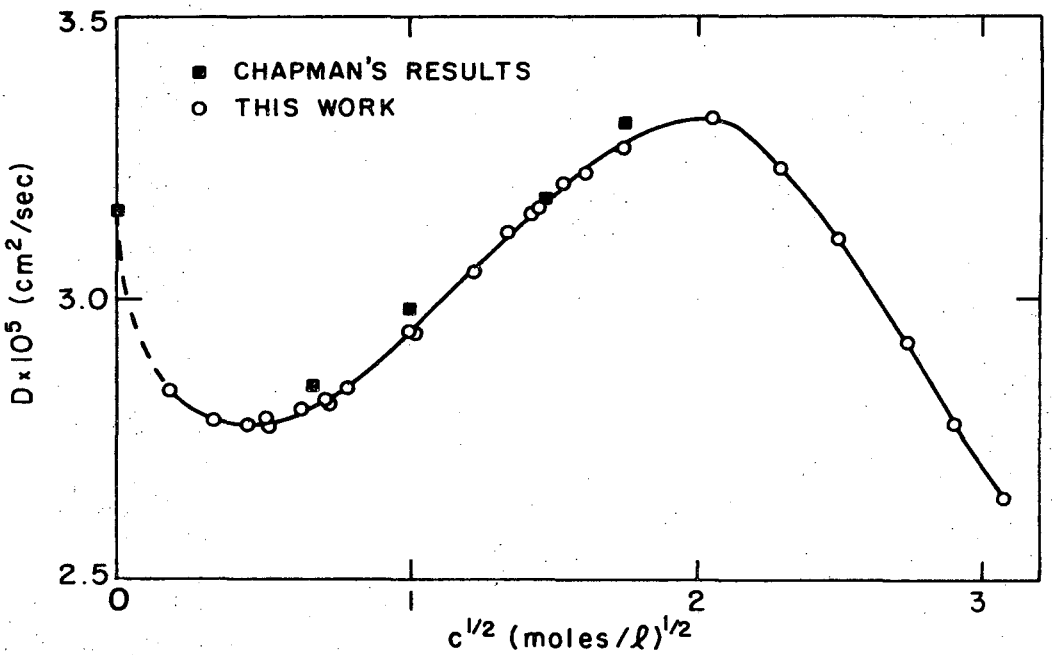

XBL 6912-6668

Fig. 5-6 The diffusion coefficient of nitric acid in water at 25°C.

Table 5-1, several exceptional runs are characterized by larger errors in the diffusion coefficient. In almost all such runs we had to contend with a relatively smaller number of fringe shift measurements because we either had to discard some points which did not conform with the fit line, or we were limited to a short time period when relevant readings could be taken such as in dilute solutions.

A major source of error was due to the analytical method by which final concentrations were determined. In concentrated solutions an error of one percent in concentration would correspond to an error of about 0.1 percent in the diffusion coefficient. This error would become more pronounced at low concentrations especially when one has to account for the difference between the actual end-point in acid-base titrations and the apparent end point of phenolphthalein.

2. Viscosities

Viscosities and densities of nitric acid were measured at concentrations 0 to 1 molar in order to extend the available viscosity data to the low concentration range. Densities of the sample solutions had to be measured accurately because they constitute an important factor in calculating the viscosities from viscosimeter readings.

Instead of measuring the sample concentrations by titration, we chose to compute them from our density data using reliable and accurate concentration - density data reported in the literature.[23] We fitted the literature data with an appropriate correlation function (see Appendix). We then calculated the concentrations iteratively from this function. The results are presented in Table 5-2. Measurement of viscosities in dilute solutions significantly improved our viscosity correlation for nitric acid

TABLE 5-2 The viscosity of nitric acid in water at 25°C

c(moles/ℓ)	ρ(g/cc)	η (cp")
0.0941	1.0002	0.8754
0.2024	1.0038	0.8799
0.2896	1.0067	0.8852
0.4914	1.0134	0.8945
0.6000	1.0170	0.8995
0.6816	1.0197	0.9038
0.8026	1.0237	0.9081
0.8813	1.0263	0.9138
0.9875	1.0298	0.9155

because in the absence of such data the correlation function anomalously exhibits a maximum for viscosity at about 0.2 molar.

3. Ionic and Thermodynamic Diffusion Coefficients

The experimental diffusion coefficient of nitric acid is found to go through a minimum at about 0.2 molar, increase to a maximum value at around 4 molar and then decrease continuously at higher concentrations. This trend in the measured diffusion coefficient is in qualitative agreement with the behavior of other strong acids in aqueous solution. One can thus speculate about the microscopic nature of nitric acid solutions with the aid of knowledge gathered from studies on the behavior of hydrogen and nitrate ions in water and the known characteristics of other strong acids in aqueous solution. Without such information the differential diffusivity data is hardly indicative of the actual diffusion mechanism in nitric acid solutions. Since the thermodynamic diffusion coefficient is relatively independent of concentration, as Eq. (2-21) suggests, the behavior of the measured diffusivity is largely controlled by the activity coefficient.

In order to obtain a more realistic description of interactions between the individual ions and the solvent molecules, we should investigate the behavior of the $\mathfrak{D}_{ij}$ coefficients with the aid of equations developed in Chapter II. For this purpose we converted the available density, viscosity, conductivity, transference number, diffusivity and activity coefficient data to a consistent set of units and fitted them with empirical correlation functions. Coefficients of the fit functions are tabulated in the Appendix. We present the smoothed data in Table 5-3. We then computed the thermodynamic and ionic diffusion coefficients. The results are listed in Table 5-4 and depicted in Figs. 5-7 and 5-8.

TABLE 5-3 Selected transport and thermodynamic properties of nitric acid in water at 25°C.

c	ρ	η	Λ^*	t_+	D	$1 + \frac{d\ln\gamma}{d\ln m}$
0.	.9971	.8903	421.27	.8304	3.158	1.0000
.001	.9971	.8906	416.68	.8322	3.099	.9853
.002	.9971	.8907	414.88	.8328	3.077	.9799
.005	.9972	.8909	411.45	.8341	3.036	.9703
.010	.9974	.8912	407.81	.8354	2.995	.9610
.020	.9977	.8915	403.02	.8370	2.945	.9503
.050	.9987	.8922	394.50	.8394	2.869	.9363
.100	1.0004	.8929	386.04	.8411	2.814	.9294
.200	1.0037	.8939	375.28	.8419	2.778	.9325
.300	1.0070	.8948	367.43	.8415	2.777	.9431
.500	1.0136	.8965	354.86	.8394	2.808	.9727
.700	1.0202	.8983	344.00	.8366	2.855	1.0075
1.000	1.0301	.9013	328.97	.8323	2.932	1.0650
1.500	1.0466	.9072	305.31	.8254	3.053	1.1694
2.000	1.0631	.9144	282.69	.8192	3.151	1.2815
2.500	1.0793	.9229	261.06	.8134	3.223	1.3989
3.000	1.0955	.9325	240.52	.8081	3.269	1.5193
3.500	1.1115	.9434	221.19	.8029	3.292	1.6400
4.000	1.1273	.9555	203.12	.7977	3.294	1.7579
4.500	1.1429	.9689	186.34	.7924	3.277	1.8694
5.000	1.1583	.9835	170.84	.7868	3.244	1.9708
6.000	1.1883	1.0167	143.52	.7743	3.141	2.1267
7.000	1.2172	1.0553	120.73	.7595	3.003	2.1942
8.000	1.2448	1.0997	101.87	.7415	2.844	2.1505
10.000	1.2959	1.2080	73.70	.6941	2.514	1.7249

*Equivalent conductivity.

TABLE 5-4 Calculated transport properties of nitric acid in water at 25°C.

c	$\mathcal{D}_{o+}$	$\mathcal{D}_{o-}$	$\mathcal{D}_{+-}$	$\mathcal{D}$
0.	9.310	1.901	0.	3.158
.001	9.337	1.881	1.711E-07	3.131
.002	9.346	1.873	2.424E-07	3.121
.005	9.364	1.858	3.849E-07	3.102
.010	9.380	1.844	5.485E-07	3.082
.020	9.397	1.825	7.877E-07	3.058
.050	9.408	1.796	1.303E-06	3.017
.100	9.385	1.770	1.979E-06	2.980
.200	9.283	1.743	3.191E-06	2.936
.300	9.149	1.725	4.398E-06	2.903
.500	8.836	1.693	6.991E-06	2.841
.700	8.496	1.660	9.880E-06	2.777
1.000	7.972	1.606	1.474E-05	2.672
1.500	7.115	1.503	2.382E-05	2.481
2.000	6.321	1.394	3.313E-05	2.284
2.500	5.606	1.286	4.152E-05	2.092
3.000	4.974	1.182	4.805E-05	1.911
3.500	4.421	1.087	5.214E-05	1.746
4.000	3.940	1.001	5.364E-05	1.597
4.500	3.523	.925	5.277E-05	1.466
5.000	3.164	.859	4.995E-05	1.352
6.000	2.589	.755	4.068E-05	1.169
7.000	2.167	.685	2.995E-05	1.040
8.000	1.859	.647	2.043E-05	.959
10.000	1.488	.660	8.109E-06	.920

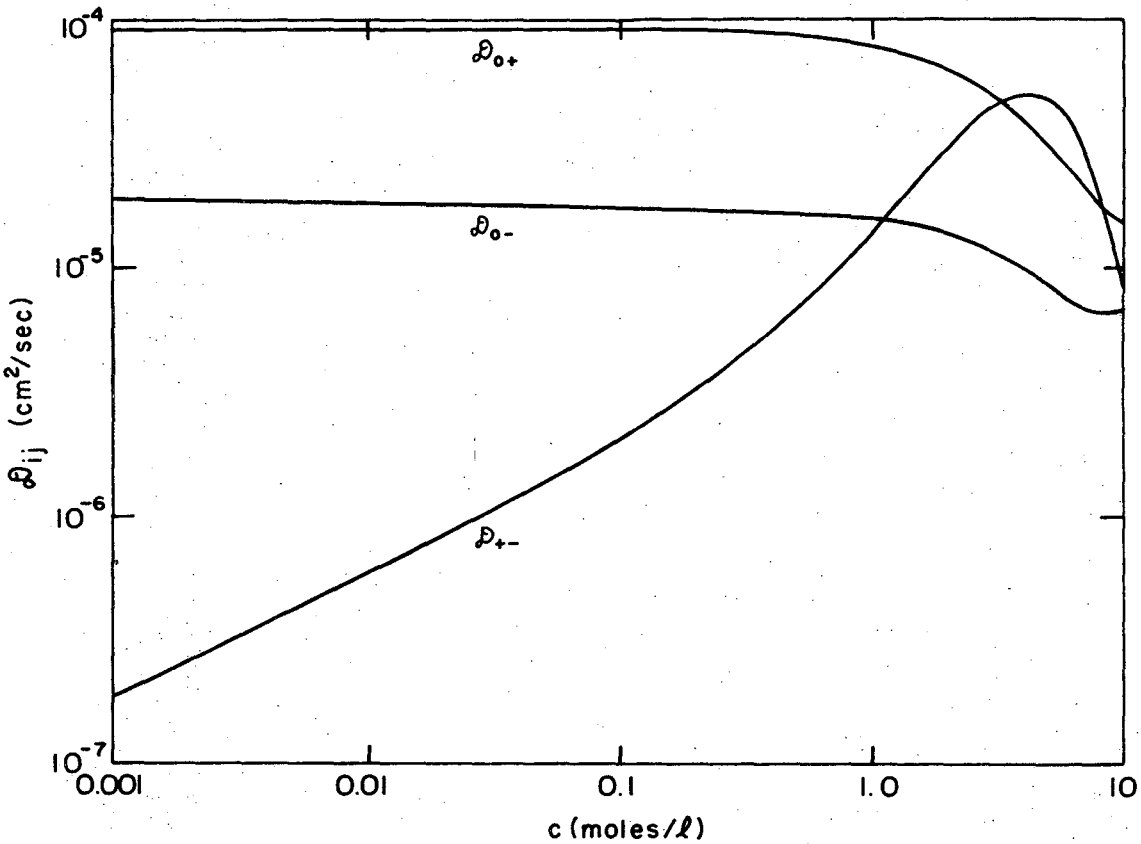

XBL 6912-6669

Fig. 5-7 The multicomponent diffusion coefficients of nitric acid in water at 25°C.

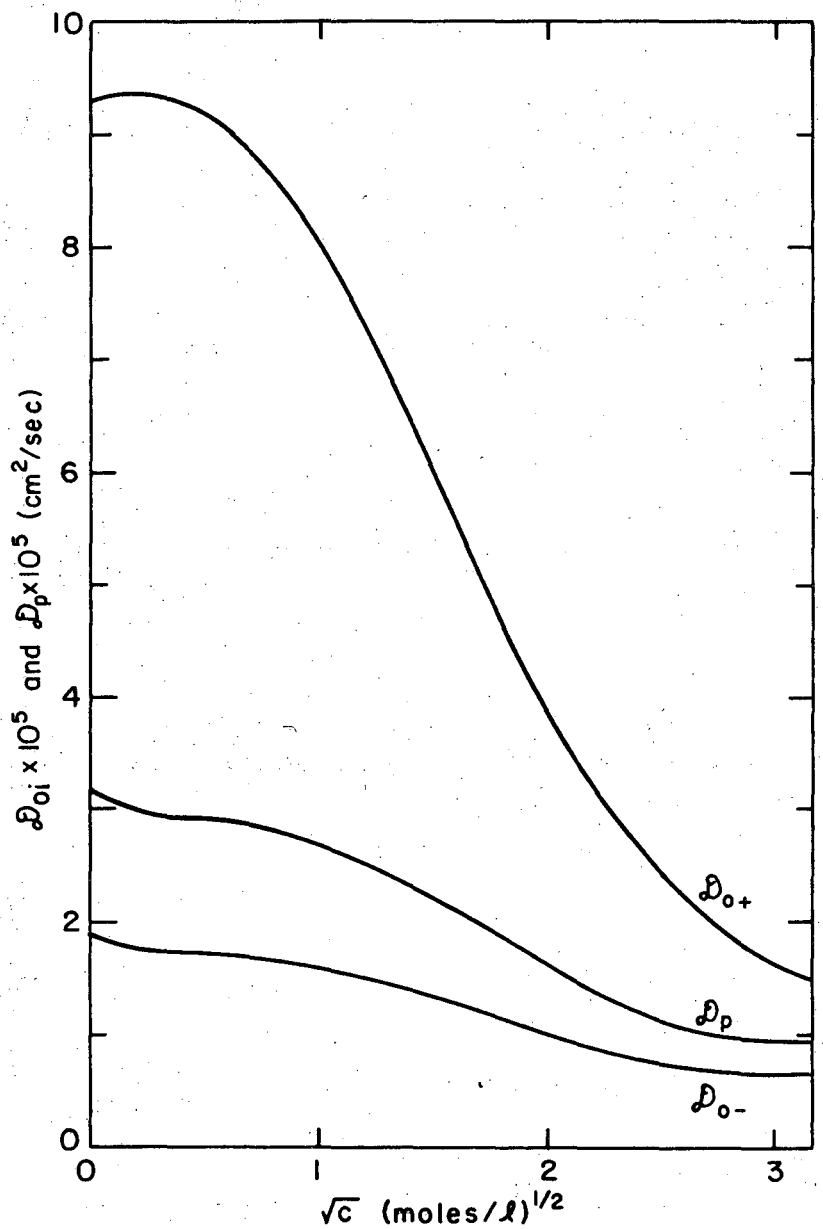

XBL 6912-6671

Fig. 5-8 The multicomponent and thermodynamic diffusion coefficients of nitric acid in water at 25°C.

The logarithmic plot shown in Fig. 5-7 represents the behavior of the $\mathcal{D}_{ij}$ coefficients particularly at low concentrations. The quantity $\mathcal{D}_{+-}$, which vanishes at zero concentration, increases by many orders of magnitude with concentration due to electrostatic attractions between oppositely changed ions. It reaches a maximum at about 4 molar, which also corresponds to the maximum in the measured diffusion coefficient. It then decreases at a fast rate as the mean distance between the ions become small enough to initiate ionic association.

The $\mathcal{D}_{oi}$ coefficients represent the interaction of solute ions with the solvent molecules. Diffusivity of the hydrogen ion $\mathcal{D}_{o+}$ is considerably larger than the diffusion coefficient of the nitrate ion demonstrating relatively high mobility of the hydrogen ion in aqueous solution. The $\mathcal{D}_{oi}$ coefficients do not vary from their limiting values to any appreciable extent as long as the solution remains dilute. At concentrations above one molar we observe that the $\mathcal{D}_{oi}$ values undergo significant changes.

We plotted the $\mathcal{D}_{oi}$ coefficients on a linear scale in Fig. 5-8 in order to obtain a more detailed picture of their behavior at large concentrations. The concentration dependence of the thermodynamic diffusion coefficient is also depicted. We observe that the diffusion coefficient of the hydrogen ion goes through a simple maximum and then decreases rapidly at high concentrations. The high mobility of this ion in dilute solutions is attributed to fast proton transfer between water molecules and the hydrogen ions. At higher concentrations, the structure making ability of the hydrogen ion is the dominating factor. Hydrogen is strongly structure-making because it carries a large charge relative to its size and therefore undergoes a high degree of solvation with the water molecules. The presence

of hydrogen ions even obscures the structure-breaking effect of the bulkier nitrate ion. The diffusion coefficient of the nitrate ion is thus forced to decrease gradually with concentration.

The effect of nitric acid on the structure of water is then on the average that of increased order as reflected by the monotonical decrease in the thermodynamic diffusion coefficient and a corresponding increase in the viscosity. We have also seen that the $\mathfrak{D}_{ij}$ coefficients and the thermodynamic diffusion coefficient provide a systematic description of transport mechanism in nitric acid solutions compared to what we could learn from the behavior of measured quantities such as the differential diffusion coefficient.

VI. CONCLUSIONS AND RECOMMENDATIONS

We have presented a set of fundamental relationships of transport in electrolytic solutions, which apply to both dilute and concentrated systems. These flux equations offer systematic and consistent definitions for various transport properties which are conveniently related to experimentally measureable quantities. We have seen that these relationships facilitate the formulation and analysis of mass transfer problems, particularly in concentrated solutions, such as the problem of restricted diffusion. They also provide the basis for the correlation of transport data and calculation of more meaningful parameters such as the thermodynamic and ionic diffusion coefficients. We have observed in our study of diffusion in nitric acid solutions that the thermodynamic diffusion coefficient provides a more realistic description of transport in concentrated solutions than the measured diffusivity. The ionic coefficients supply us with clues in understanding the mechanism of particulate diffusion in solution and the effects of various ions on the microscopic structure of water.

The macroscopic nature of the basic equations limit the number of relationships between the transport properties compared to the quantity of all the independent parameters defined. In order to obtain a complete description of transport in an electrochemical system, one either has to derive additional relationships from microscopic considerations or measure some of the unknown properties experimentally. We have proposed a few methods of correlating and predicting diffusion coefficients in binary solutions. Equation (3-2) follows directly from the regular solution assumptions, but predicts quite accurately the diffusion coefficient

of alkali halides with the exception of the iodides and the lithium halides. We derived a one parameter rate quation for the diffusion coefficient, which amounts for the activity and electrophoretic corrections, using a simple lattice model for an electrolyte solution. This equation correlates experimental diffusivity data within a few percent. The precision is less for the polyvalent systems. The same equation can be employed to predict diffusion coefficients over a wide concentration range if one or two experimental data points are available. We made an attempt to extend the rate equation to systems without any experimental diffusivity data and which do not obey the assumption of Eq. (3-2) at high concentrations. We thus tried to predict diffusion coefficients for these systems from low concentration viscosity data. Predicted values agreed satisfactorily with the experimental data as long as viscosity data were available at low concentrations. Unfortunately, most of the viscosity data reported in the literature have been obtained at high concentrations.

We discussed the controversy about the definition of the thermodynamic diffusion coefficient encountered in the literature. We could not arrive at a definite conclusion whether $\mathcal{D}_p$ or $\mathcal{D}_x$ provides a more convenient definition of the thermodynamic diffusion coefficient. The choice of either convention in our theoretical treatments was based on purely empirical grounds. Our observations seem to indicate, however, that $\mathcal{D}_x$ is more sensitive to ionic association in concentration solutions.

The methods we proposed to estimate diffusion coefficients in concentrated solutions carry a number of assumptions which may seem ambiguous in view of the complicated behavior of electrolytic systems. Their agreement with the experimental data is nevertheless satisfactory, and they can therefore be employed as tentative tools to estimate diffusion coeffi-

cients until more rigorous treatments of the microscopic theories yield better descriptions of the transport properties. Chapman's efforts[7] to predict the quantity $\mathcal{D}_{+-}$ may turn fruitful upon more realistic assumptions and the introduction of the electrophoretic terms. The corresponding states theory may also lead to further progress in this field. Good agreement between theory and experiment has been obtained for transport in fused salts[41]. Existing statistical mechanical theories for fused salts may be modified by introducing approximations appropriate for electrolytic solutions, and with the application of the corresponding states theory it may be possible to obtain correlations of transport properties. References 21, 35 and 41 may provide some guidance.

Our theoretical study indicated that additional experimental data are necessary for further progress in the development of reliable quantitative correlations of the transport properties. We attempted to provide some of the requisite data by measuring diffusivities and viscosities. We employed the restricted diffusion cell and Rayleigh interferometry for the measurement of diffusion coefficients. This method provides a few advantages. Its mathematical analysis involves very few assumptions. It does not require an initially sharp boundary between two solutions because the initial conditions have been left as arbitrary in the analysis of the problem. Dimensions of the optical cell are sufficiently small so that the diffusing solutions are not significantly affected by convection. The method yields accurate diffusion coefficients with estimated errors not exceeding 0.2 percent in concentrated solutions. In dilute systems the accuracy drops considerably; one might resort back to Harned's original conductimetric method at low concentrations. One disadvantage is that the time required

for each data point is several days. The analytical method for the determination of final concentrations should also be improved. A conductimetric or potentiometric titration method could be tried for future experiments to acquire higher accuracy in concentration, especially in dilute solutions.

APPENDIX

Functions Used to Fit Thermodynamic and Transport Property Data on Electrolytic Solutions

Experimental data[15] on the thermodynamic and transport properties of various electrolytic systems were fitted to certain correlation functions by Newman[27] in order to interpolate the experimental data to the concentration where a calculation was made. We used some of his results in Chapt. II. We also used a computer program written by Newman[29] to convert all available experimental data on the properties of nitric acid to a consistent set of units and fit them to these functions. The functions are given by

$$\rho = \exp\left(a_1 + a_2 c + a_3 c^{3/2} + a_4 c^2\right) \tag{A-1}$$

for densities,

$$\eta = \exp\left(b_1 + b_2 c^{1/2} + b_3 c + b_4 c^{3/2} + b_5 c^2\right) \tag{A-2}$$

for viscosities,

$$t_+ = d_1 + d_2 c^{1/2} + d_3 c + d_4 c^{3/2} + d_5 c^2 \tag{A-3}$$

for the cation transference numbers, and

$$P = \exp\left(e_1 + \frac{e_2 c^{1/2}}{1+c^{1/2}} + e_3 c + e_4 c^{3/2} + e_5 c^2\right) \tag{A-4}$$

for the equivalent conductances, diffusion coefficients and the properties $\mathfrak{D}_{oi}$, $\mathfrak{D}$ and $\mathfrak{D}_{+-}/\sqrt{c}$.

The activity coefficient data from each literature source were fitted separately to the function,

$$\gamma = \exp\left(f_1 + \frac{f_2 m^{1/2}}{1 + m^{1/2}} + f_3 m + f_4 m^{3/2} + f_5 m^2 + f_6 m^3\right). \tag{A-5}$$

The results were differentiated and combined to calculate $(1 + d\ln\gamma/d\ln m)$ values. These were then correlated by

$$1 + \frac{d\ln\gamma}{d\ln m} = \exp\left(0.5\, g_2 \frac{c^{1/2}}{(1 + c^{1/2})^2} + g_3\, c + 1.5\, g_4\, c^{3/2} + 2g_5 c^2 + 3g_6 c^3\right) \qquad \text{(A-6)}$$

The coefficients of functions, which are used in Chapt. II to calculate densities, viscosities and $(1 + d\ln\gamma/d\ln m)$ values for the electrolyte systems studied are given in Tables A-1, A-2 and A-3 in digital computer notation. In Table A-4 we tabulated the coefficients of each function for nitric acid as the results of our correlation of thermodynamic and transport property data in Chapt. V.

TABLE A-1 Density function coefficients for aqueous electrolytic solutions at 25°C

Solute	a_1	a_2	a_3	a_4
$CaCl_2$	-2.9343E-03	9.2262E-02	-7.0074E-03	-2.0286E-03
CsCl	-2.9343E-03	1.3887E-01	-1.8255E-02	-1.9451E-04
HCl	-2.9343E-03	1.8333E-02	-7.3222E-04	-1.3689E-04
KBr	-2.9343E-03	8.7612E-02	-6.0088E-03	-1.2023E-03
KCl	-2.9343E-03	4.8293E-02	-2.8926E-03	-5.6717E-04
KI	-2.9343E-03	1.2922E-01	-1.5403E-02	-4.5300E-04
LiCl	-2.9343E-03	2.6891E-02	-3.1238E-03	2.5432E-04
NH_4Cl	-2.9343E-03	1.8036E-02	-1.9914E-03	5.0595E-05
NaCl	-2.9343E-03	4.2867E-02	-3.3378E-03	-2.2160E-04

TABLE A-2 Viscosity function coefficients for aqueous electrolytic solutions at 25°C

Solute	b_1	b_2	b_3	b_4	b_5
$CaCl_2$	-1.1620E-01	-1.5493E-02	4.1776E-01	-1.9943E-01	9.2589E-02
CsCl	-1.1620E-01	-4.7026E-02	6.3195E-02	-7.6271E-02	2.7516E-02
HCl	-1.1620E-01	5.5179E-03	6.2265E-02	-9.5680E-03	2.6976E-03
KBr	-1.1620E-01	1.9828E-03	-4.2307E-02	-3.6369E-03	1.2553E-02
KCl	-1.1620E-01	6.6926E-03	-2.0336E-02	5.1054E-03	6.2871E-03
KI	-1.1620E-01	-3.1544E-03	7.8326E-02	-1.4011E-03	1.7117E-02
LiCl	-1.1620E-01	-7.2424E-03	1.9391E-01	-5.8170E-02	1.6532E-02
NH_4Cl	-1.1670E-01	2.2917E-02	-6.6649E-02	4.1177E-02	-5.5124E-03
NaCl	-1.1620E-01	8.2901E-03	7.4043E-02	-6.1218E-04	9.5181E-03

TABLE A-3 $(1 + d\ln\gamma/d\ln m)$ function coefficients for aqueous electrolytic solutions at 25°C

Solute	g_2	g_3	g_4	g_5	g_6
$CaCl_2$	-2.4515E+00	7.9379E-01	-1.5193E-01	2.6538E-02	-2.6085E-03
CsCl	-1.2303E+00	1.4581E-01	1.1964E-01	-2.1628E-02	2.4710E-05
HCl	-1.0995E+00	3.7489E-01	-4.2364E-02	-1.0586E-03	-1.3064E-05
KBr	-1.1153E+00	8.6687E-02	-4.4777E-02	2.0851E-02	-1.1321E-03
KCl	-1.1537E+00	1.0704E-01	-9.5361E-02	4.3579E-02	-2.3600E-03
KI	-1.0767E+00	1.6609E-01	-1.1519E-01	5.2317E-02	-3.8288E-03
LiCl	-1.0342E+00	2.5368E-01	2.2279E-02	-1.0540E-02	-1.8174E-06
NH_4Cl	-1.1134E+00	2.8013E-02	1.1234E-03	5.0969E-03	-7.6323E-04
NaCl	-1.1052E+00	1.4989E-01	-5.0404E-02	2.1882E-02	-9.5854E-04

TABLE A-4. Correlation function coefficients for thermodynamic and transpart properties of aqueous nitric acid solutions at 25°C. σ is the average error in the least squares fit.

Property						
ρ	a_1	a_2	a_3	a_4		$\sigma(\%)$
	-2.9343E-3	3.2827E-2	6.8615E-4	-8.7830E-4		0.02
η	b_1	b_2	b_3	b_4	b_5	
	-1.1620E-1	1.0669E-2	-7.2668E-3	7.9462E-3	9.2850E-4	1.39
t_+	d_1	d_2	d_3	d_4	d_5	
	8.3040E-1	5.8115E-2	-8.8519E-2	3.9018E-2	-6.6872E.3	0.16
	e_1	e_2	e_3	e_4	e_5	
Λ	6.0433E+0	-3.5787E-1	1.6790E-2	-1.0059E-1	1.5417E-2	0.43
D	-1.0363E+1	-6.2455E-1	4.0399E-1	-1.8720E-1	2.1263E-2	0.35
$\mathfrak{D}$	-1.0363E+1	-2.8427E-1	1.8022E-1	-2.5905E-1	5.3718E-2	0.66
$\mathfrak{D}_{0+}$	-9.2818E+0	9.6192E-1	-1.1785E-1	-1.1433E-1	2.8874E-2	0.76
$\mathfrak{D}_{0-}$	-1.0870E+1	-3.6376E-1	2.4703E-1	-2.9498E-1	6.0766E-2	0.69
$\mathfrak{D}_{+-}/\sqrt{c}$	-1.2128E+1	-3.6960E-2	1.8242E+0	-8.9694E-1	9.4033E-2	13.11
	g_2	g_3	g_4	g_5	g_6	
$1+\frac{d\ln\gamma}{d\ln m}$	-1.0069E+0	1.8478E-1	6.3601E-3	-2.2222E-3	-3.5600E-4	2.11

NOMENCLATURE

A, B	constants in Eq. (4-22)
A'	$A\sqrt{3}$
a	ion size parameter (Å) (Chapter III)
a	height of restricted diffusion cell (cm) (Chapter IV)
a_e	activity coefficient of the electrolyte in binary solution
a_i, b_i, d_i, e_i, f_i, g_i	coefficients of correlation functions given in the Appendix
c	concentration of binary electrolyte (moles/cm^3)
c_o	concentration of solvent (moles/cm^3)
c_i	concentration of species i (moles/cm^3)
c_T	total solution concentration (moles/cm^3)
D	differential diffusion coefficient (cm^2/sec)
$\mathfrak{D}_{ij}$	multicomponent diffusion coefficient (cm^2/sec) (Eq. (2-4).
$\mathfrak{D}$	thermodynamic diffusion coefficient (cm^2/sec)
d	spacing between the slits of an interferometer (cm)
e	electronic charge (Coulombs)
F	Faraday's constant (Coulomb/equiv.)
ΔF_o^*	activation free energy of transition (joule/mole)
h	Planck's constant (erg-sec)
$\underline{i}$	current density (amp/cm^2)
$\underline{J}_s^*$	molar flux of salt relative to the molar average velocity (moles/cm^2-sec)
K	parameter defined by Eq. (3-19)
k	specific reaction rate for diffusion (sec^{-1})

k	Boltzmann's constant (erg/°K)
k_D	kT/h
ℓ	thickness of medium through which light passes to generate interference (cm)
m	molality
m	order of interference fringe (Chapter IV)
n	total number of particles in solution which interact with a single water molecule
n_i	np_i
$\underline{N}_i$	flux of species i (moles/cm^2-sec)
N_{Avo}	Avogadro's Number
P	property given by Eq. (A-4)
p_i	particle fraction of species i ($= \frac{c_i}{c_o + \nu c}$)
q	constant defined in Eq. (3-16)
q'	constant defined in Eq. (3-21)
R	universal gas constant (joule/mole °K)
R_i	rate of homogeneous generation of species i (moles/cm^3-sec)
T	temperature (°K)
t	time
t_i	transference number of species i with respect to the solvent velocity
$\bar{V}_o$	partial molar volume of solvent (cm^3/mole)
$\underline{v}$	mass average fluid velocity (cm/sec)
$\underline{v}_i$	mass average velocity of species i (cm/sec)
$\underline{v}_o$	mass average velocity of solvent (cm/sec)
$\underline{v}^*$	molar average fluid velocity (cm/sec)

x_i	mole fraction of species i ($= \frac{c_i}{c_o + c}$)
y	position coordinate in the restricted diffusion cell (cm)
z	position coordinate in Eq. (3-3)
z_i	valence of species i
γ	mean molal activity coefficient
Δ_1, Δ_2	electrophoretic terms
δ_i	perturbation of the activation energy of water caused by a single particle of species i (joule/mole)
ϵ	dielectric constant (Chapter III)
ϵ	perturbation parameter (Chapter IV)
κ	specific conductance (mho/cm)
λ	wavelength of light (Chapter IV)
λ	jump distance of a diffusing molecule (cm)(Chaper III)
μ_i	electrochemical potential of species i (joule/mole)
μ	refractive index (Chapter IV)
η	viscosity (centipoise)
ν	$\nu_+ + \nu_-$
ν_+, ν_-	numbers of cations and anions produced by dissociation of one molecule of electrolyte
ρ	density of solution (gm/cm^3)

Superscripts

o	property at infinite dilution
∞	value at infinite time
(i)	identifies coefficients of terms in singular perturbation expansion series (Chapter IV)

Subscripts

o	property of solvent

s	property of salt
e	property of electrolyte
+, -	properties of cations and anions
x	defined in terms of mole fraction
p	defined in terms of particle fraction
f	in the forward direction
b	in the backward direction

ACKNOWLEDGEMENTS

I would like to express my gratitude to Professor John Newman for his guidance and criticism in all phases of this project.

This work was supported jointly by the United States Atomic Energy Commission and the Petroleum Research Fund, administered by the American Chemical Society.

REFERENCES

1. R. J. Bearman, On the Molecular Basis of Some Current-Theories of Diffusion, J. Phys. Chem. 65, 1961 (1961).

2. R. N. Bhatia, K. E. Gubbins and R. D. Walker, Mutual Diffision in Concentrated Aqueous Potassium Hydroxide Solutions, Trans. Farad. Soc. 64, 2091 (1968).

3. R. B. Bird, W. E. Stewart and E. N. Lightfoot, Transport Phenomena (Wiley, New York, 1966), p. 502.

4. Ibid, p. 570.

5. T. W. Chapman, The Transport Properties of Concentrated Electrolytic Solutions (Ph.D. Thesis), UCRL-17768, Nov. 1967.

6. Ibid., p.27.

7. Ibid., Chapter 4.

8. Ibid., p. 35.

9. Ibid., Chapter 5, Sections B, C and D.

10. Ibid., Appendix C.

11. Ibid., p. 110.

12. Ibid., Chapter 6.

13. Ibid., p. 125.

14. Ibid., p. 128.

15. T. W. Chapman and J. Newman, A Compilation of Selected Theromdynamic and Transport Properties of Binary Electrolytes in Aqueous Solutions, UCRL-17707, May 1968.

16. S. Glasstone, K. J. Laidler and H. Eyring, The Theory of Rate Processes (McGraw Hill, New York, 1941), p. 516.

17. Ibid., p. 184.

18. K. E. Gubbins, K. K. Bhatia and R. D. Walker, Jr., Diffusion of Gases in Electrolytic Solutions, A. I. Che. E. J. 5, 548 (1966).

19. H. S. Harned and D. M. French A Conductance Method for the Determination of the Diffusion Coefficients of Electrolytes, Ann. N.Y. Acad. Sci. 46, 267 (1945).

20. G. S. Hartley and J. Crank, Some Fundamental Definitons and Concepts in Diffusion Processes, Trans. Farad. Soc. 45, 801 (1949).

21. E. Helfand and S. A. Rice, Principle of Corrsponding States for Transport Properties, J. Chem. Phys. 32, 1642 (1960).

22. L. Hsueh, Diffusion and Migration in Electrochemical Systems (Ph.D. Thesis), UCRL-18597, Dec. 1968.

23. International Critical Tables, 3, 58 (1928).

24. E. Jahnke and F. Emde, Tables of Functions, (Dover, New York, 1945).

25. H. S. Mickley, T. K. Sherwood and C. E. Reid, Applied Mathematics in Chemical Engineering, 2nd Ed. (McGraw Hill, New York, 1957).

26. P. Milios, A Theoretical Analysis of the Moving Boundary Measurement of Transference Numbers (M.S. Thesis) UCRL-17807, Spet. 1967.

27. J. Newman, D. Bennion and C. W. Tobias, Mass Transfer in Concentrated Binary Electrolytes, Ber. Bunsenges. Physik. Chem. 69, 608 (1965).

28. J. Newman, Transport Processes in Electrolytic Solutions, in Advances in Electrochemistry and Electrochemical Engineering, edited by C. W. Tobias, (Interscience, New York, 1967), Vol. 5, p. 87.

29. J. Newman (Dept. of Chemical Engineering, University of California, Berkeley, California), private communication, 1969.

30. L. Onsager and R. M. Fuoss, Irreversible Processes in Electrolytes. Diffusion, Conductance and Viscous Flow in Arbitrary Mixtures of

Strong Electrolytes, J. Phys. Chem. 36, 2689 (1932).

31. R. J. Podolsky, Transport Processes in Electrolyte Solutions, J. Am. Chem. Soc. 80, 4442 (1958).

32. J. E. Prue, Ion Association and Solvation in Chemical Physics of Ionic Solutions, edited by R. E. Conway and R. G. Barradas (Wiley, New York, 1966), p. 163.

33. G. A. Ratcliff and J. G. Holdcroft, Diffusivities of Gases in Aqueous Electrolyte Solutions, Trans. Inst. Chem. Eng. 41,315 (1963).

34. O. Redlich, W. E. Gargrave and W. D. Krostek, Thermodynamics of Solutions: Consistency of Sparce Data. Activities of Nitric and Perchloric Acids, Ind. Eng. Chem. Fund. 7, 211 (1968).

35. H. Reiss and S. W. Mayer, Law of Corresponding States for Fused Salts, J. Chem. Phys. 35, 820 (1961).

36. R. A. Robinson and R. H. Stokes, Electrolyte Solutions, 2nd Ed., Rep. and Rev. (Butterworths, London, 1968), p.156.

37. Ibid., p. 327.

38. Ibid., p. 291.

39. Ibid., p. 246.

40. R. H. Stokes, The Electrophoretic Corrections to the Diffusion Coefficient of an Electrolyte Solution, J. Am. Chem. Soc. 75, 4563 (1953).

41. L. R. White and H. T. Davis, Thermal Conductivity of Molten Alkali Nitrates, J. Chem. Phys. 47, 5433 (1967).

42. R. Lühdemann, Über die Konzentrationsabhangigkeit der Aquivalentrefraktion einiger Salze und Sauren in wasserigen Lösung, Z. Physik Chem. 29, 133 (1935).

LEGAL NOTICE

This report was prepared as an account of Government sponsored work. Neither the United States, nor the Commission, nor any person acting on behalf of the Commission:

A. Makes any warranty or representation, expressed or implied, with respect to the accuracy, completeness, or usefulness of the information contained in this report, or that the use of any information, apparatus, method, or process disclosed in this report may not infringe privately owned rights; or

B. Assumes any liabilities with respect to the use of, or for damages resulting from the use of any information, apparatus, method, or process disclosed in this report.

As used in the above, "person acting on behalf of the Commission" includes any employee or contractor of the Commission, or employee of such contractor, to the extent that such employee or contractor of the Commission, or employee of such contractor prepares, disseminates, or provides access to, any information pursuant to his employment or contract with the Commission, or his employment with such contractor.

TECHNICAL INFORMATION DIVISION
LAWRENCE RADIATION LABORATORY
UNIVERSITY OF CALIFORNIA
BERKELEY, CALIFORNIA 94720